ORNL/TM-2022/2650

Interim Report on FY22 ORNL A709 Welding Research and Testing of Production Welds in Support of Developing ASME A709 Code Case Data Package

Zhili Feng
Yiyu Wang
Doug Kyle
Yanli Wang

Approved for public release.
Distribution is unlimited.

September 2022

OAK RIDGE National Laboratory

ORNL IS MANAGED BY UT-BATTELLE LLC FOR THE US DEPARTMENT OF ENERGY

DOCUMENT AVAILABILITY

Reports produced after January 1, 1996, are generally available free via OSTI.GOV.

Website www.osti.gov

Reports produced before January 1, 1996, may be purchased by members of the public from the following source:

National Technical Information Service
5285 Port Royal Road
Springfield, VA 22161
Telephone 703-605-6000 (1-800-553-6847)
TDD 703-487-4639
Fax 703-605-6900
E-mail info@ntis.gov
Website http://classic.ntis.gov/

Reports are available to US Department of Energy (DOE) employees, DOE contractors, Energy Technology Data Exchange representatives, and International Nuclear Information System representatives from the following source:

Office of Scientific and Technical Information
PO Box 62
Oak Ridge, TN 37831
Telephone 865-576-8401
Fax 865-576-5728
E-mail reports@osti.gov
Website https://www.osti.gov/

This report was prepared as an account of work sponsored by an agency of the United States Government. Neither the United States Government nor any agency thereof, nor any of their employees, makes any warranty, express or implied, or assumes any legal liability or responsibility for the accuracy, completeness, or usefulness of any information, apparatus, product, or process disclosed, or represents that its use would not infringe privately owned rights. Reference herein to any specific commercial product, process, or service by trade name, trademark, manufacturer, or otherwise, does not necessarily constitute or imply its endorsement, recommendation, or favoring by the United States Government or any agency thereof. The views and opinions of authors expressed herein do not necessarily state or reflect those of the United States Government or any agency thereof.

ORNL/TM-2022/2650

Materials Science and Technology Division

INTERIM REPORT ON FY22 ORNL A709 WELDING RESEARCH AND TESTING OF PRODUCTION WELDS IN SUPPORT OF DEVELOPING ASME A709 CODE CASE DATA PACKAGE

Zhili Feng
Yiyu Wang
Doug Kyle
Yanli Wang

September 2022

Prepared by
OAK RIDGE NATIONAL LABORATORY
Oak Ridge, TN 37831
managed by
UT-BATTELLE LLC
for the
US DEPARTMENT OF ENERGY
under contract DE-AC05-00OR22725

CONTENTS

LIST OF FIGURES

LIST OF TABLES

ACRONYMS

ART	Advanced Reactor Technologies
ASME	The American Society of Mechanical Engineers
ASTM	American Society for Testing and Materials. (aka, ASTM International)
DOE	Department of Energy
ESR	Electroslag Remelting
FR	Fast Reactors
FL	Fusion Line
GTAW	Gas Tungsten Arc Welding
HAZ	Heat Affected Zone
ORNL	Oak Ridge National Laboratory
SFR	Sodium Fast Reactor
SRF	Stress Reduction Factors
SA	Solution Annealed
TIG	Tungsten Inert Gas

ACKNOWLEDGMENT

This research was sponsored by the United States (U.S.) Department of Energy (DOE) under Contract No. DE-AC05-00OR22725 with Oak Ridge National Laboratory (ORNL), which is managed and operated by the UT– Battelle LLC. Programmatic direction was provided by the Office of Nuclear Reactor Deployment of the DOE Office of Nuclear Energy.

The authors gratefully acknowledge the support provided by Sue Lesica, Federal Materials Lead for the Advanced Reactor Technologies (ART) Program; Brian Robinson, Federal Manager, ART Fast Reactors (FR) Campaign; Bo Feng of Argonne, National Technical Director, ART FR Campaign, and T.-L. Sham of Idaho National Laboratory, Technology Area Lead, Advanced Materials, ART Program.

The authors also wish to thank ORNL staff members Jeremy Moser and Brad Hall for carrying out the experiments on mechanical properties. The time spent by Lianshan Lin and Jian Chen of ORNL reviewing this report is acknowledged.

ABSTRACT

As part of the Alloy 709 ASME Code Case development effort under the Advanced Reactor Technologies (ART) Program, this work covers the development of the technical basis for weld fabrication and weld qualification of Alloy 709. This report summarizes the Alloy 709 welding research conducted at Oak Ridge National Laboratory (ORNL) in FY 2022.

Two new production welds were fabricated on two commercial heats of Alloy 709 of different phosphorus (P) levels using Alloy 709 filler metal with P content less than 20 wppm with gas tungsten arc welding (GTAW). Both production welds successfully passed ASME Section IX weld qualification tests, and this concludes the Alloy 709 welding procedure development to scale up to 2-in thick plates.

In FY 2022, we also demonstrated the success in welding of high P commercial Alloy 709 plates with weld wires having higher P content at 30 wppm. A test weld fabricated with the 30 wppm weld wire on the first commercial heat (140 wppm P) passed all weld qualification tests without issues. Additionally, experiment setup and testing procedure of the circular patch weldability test has been developed, for evaluating the P effect in weld wire on solidification cracking susceptibility of Alloy 709 weld, with the preliminary results summarized in this report. Research on further relaxing the P level restriction beyond 30 wppm are planned in FY 2023.

The preliminary cross-weld creep tests results continue to show little or no creep strength reduction relative to the base metal.

1. INTRODUCTION

Advanced materials can have a significant impact on flexibility, safety, and economics of the future sodium fast reactor (SFR). This is due to innovative designs and design simplifications that could be made possible using materials with enhanced mechanical properties. Improved materials performance also impacts safety through improved reliability and greater design margins. Improved material reliability could also result in reduced down time.

Alloy 709 is an advanced nitrogen-stabilized and niobium-strengthened austenitic stainless steel. Compared to a reference construction material 316H stainless steel for SFR, Alloy 709 has enhanced creep strength, good steam oxidation resistance and hot corrosion resistance. It is an attractive candidate construction material for SFR systems. Code qualification of Alloy 709 is underway as part of the development effort under the US Department of Energy, Advanced Reactor Technologies (ART) Program (Sham & Natesan, 2017), to provide the technical basis necessary to support the regulatory requirements for structural materials required for advanced, non-light water reactors that could be deployed in the near-to-mid-term.

Welding is essential in construction of high temperature reactor structure components. The Code Case qualification of Alloy 709 would require the development of a sound technical basis for welding. It would include the development of welding guidelines with supporting testing results to fabricate ASME Section IX (ASME, 2019) qualified welds using weld wires with appropriately specified chemistry range, to eliminate solidification cracking, minimize stress relaxation cracking susceptibility, and retain the good high temperature mechanical properties, for selected heats meeting relevant ASTM/ASME chemistry specifications.

Alloy 709 is derived from NF709, i.e., TP310MoCbN (UNS S31025) specified in ASME BPVC.II SA-213/SA-213M (ASME, 2021). NF709 seamless tube was developed by Nippon Steel Corporation in

Japan for boiler tubing applications. Previous studies such as these by Nippon Steel (2013), suggested that NF709 has relatively good weldability. Alloy 709 filler metal and Alloy 625 filler metal were the two weld metals that Nippon Steel had recommended to weld seamless tubing. Performance of Alloy 709 weldment fabricated using Alloy 625 filler metal in sodium was found to be less than optimal during the Alloy 709 intermediate term testing program because of the high solubility of nickel in sodium. Weldment fabricated from Alloy 709 filler metal (the so-called matching filler metal) was found to have good sodium compatibility. However, earlier welding studies on experimental heats of Alloy 709 in plate form by the ART Program (Yamamoto, 2014) revealed potential issues of weld solidification cracking when the level of impurities such as P is high but still within the ASME BPVC.II SA-213/SA-213M (ASME, 2021). Only the weldment with very low P content (less than 20 wppm, or <0.002 wt.%) *in both the base metal (plate form) and the matching filler metal* passed the ASME Section IX weldment qualification test. While a Section IX qualified weldment was fabricated successfully, the requirement of very low P content (20 wppm) places a severe restriction.

Computational modeling with Scheil simulations of non-equilibrium solidification found that P has the most important impact on solidification behavior. Increasing levels of P from 0.002 wt.% (20 wppm) to 0.018 wt. % (180 wppm) led to a decrease in the solidus temperature of over 300 °C (Feng, Vitek, Liu, & Wang, 2018). The modeling results lead to the development of strategies to weld Alloy 709 having wide range of chemistries without weld solidification cracking to support code qualification. One of the approaches was to limit the P level of the weld wire when welding Alloy 709 base metal having relatively high P. For weld wires with high P levels, special welding procedures or innovative welding techniques may be necessary to produce code qualified welds.

A series of ASME Section IX qualified welds were successfully fabricated using the low P weld wire (<20 wppm P) on the first commercial heat (Heat 58776) Alloy 709 plates (Feng et al. 2019, 2020, 2021). It is noted that this heat Alloy 709 plates has relatively high P level of 140 wppm. In addition, through welding parameters optimization, it demonstrated the possibility of welding the Heat 58776 plates using high P weld wire (140 wppm P), although welding defects related to solidification cracking within the qualified limit could not be eliminated. The objective of this study is to research and develop suitable welding techniques that would successfully weld Alloy 709 base metal with higher P content within the limit of ASME BPVC.II SA-213/SA-213M (ASME, 2021), and evaluate the options to relax the tight restriction on P content for the weld wire.

2. MATERIALS AND SPECIMENS

2.1 ALLOY 709 BASE METAL PLATES

In collaboration with two US steel fabricators, DOE-NE ART program successfully scaled up the production of Alloy 709 in plate form from a laboratory heat of 500 lb to three commercial heats of the Alloy 709 with the commercial Heat-1 of 45,000 lb, commercial Heat-2 of 41,000 lb, and commercial Heat-3 of 38,000lb. The commercial Heat-1 plates were fabricated by G.O. Carlson Inc of Pennsylvania, whereas the second and third heats were both fabricated by Allegheny Technologies Incorporated. The plates were produced by argon-oxygen-decarburization (AOD) followed by electroslag remelted (ESR). The plates were hot rolled, and solution annealed at a minimum temperature 1150 °C.

In this report, the base metal plates used for the Alloy 709 welding research were from commercial Heat-1 and commercial Heat-2. The plates from the two heats received an additional heat treatment: 775 °C for 10 hours in air, followed by air cooling, following the heat treatment protocol by Zhang, Sham and Young, (2019).

Table 1 summarized the two Alloy 709 base metal plates with the heat number 58776 and 529900 used in this study. The chemical compositions of these two base metal plates are listed in Table 2. For comparison, the specifications for the chemical requirements of Nippon Steel NF709, TP310MoCbN, seamless tubing, with a UNS number of S31025 in ASME SA-213 (ASME, 2021) are also listed in Table 2. Both commercial heats met the specified NF709 chemical requirements. As shown in the table, the commercial Heat-1 has relatively high P level at 0.014 wt. % (140 wppm) and Commercial heat-2 has lower P level of 0.003 wt.% (30 wppm)

Table 1. Commercial heats of Alloy 709 base metal plates

Material	Commercial Heat-1	Commercial Heat-2
Fabricator	G.O. Carlson Inc	Allegheny Technologies Incorporated
Master heat number	58776	529900
Base metal Plate ID	58776-3RBC1	CG05454
Plate gage (in)	1	2
measured plate thickness, (in)	1.125	2.05
Plate Solution Heat Treatment, (°C)	1150	1150
Aging Heat Treatment	775 °C, 10 h, air cool	775 °C, 10 h, air cool

Table 2. Chemical compositions of the two commercial heat Alloy 709 base metal plates (wt %).

Element	Commercial Heat 1 (Plate 58776-3RBC1)	Commercial Heat 2 (Plate CG05454)	ASME SA-213 UNS-S31025 Specification
	(wt.%)	(wt.%)	(wt.%)
C	0.066	0.08	0.10 max
Cr	20.05	19.9	19.5–23.0
Co	0.02	0.02	–
Ni	25.14	24.6	23.0–26.0
Mn	0.9	0.9	1.50 max
Mo	1.51	1.5	1.0–2.0
N	0.152	0.15	0.10–0.25
Si	0.38	0.39	1.00 max
P	0.014	0.003	0.030 max
S	0.001	<0.001	0.030 max
Ti	0.01	<0.01	0.20 max
Nb	0.26	0.17	0.10–0.40
Al	0.02	0.02	–
B	0.003	0.004	0.002–0.010
Cu	0.06	0.06	–
Fe	Balance	Balance	Balance

2.2 ALLOY 709 FILLER METAL WELD WIRE

Previous computational solidification simulation modeling with Scheil simulations of non-equilibrium solidification found that P has the most important impact on solidification behavior. Increasing levels of P from 0.002 wt.% (20 wppm) to 0.018 wt.% (180 wppm) led to a decrease in the solidus temperature of over 300°C (Feng, Vitek, Liu, & Wang, 2018). That is, high levels of P lead to very large increases in the non-equilibrium solidification temperature range. Thus, P is expected to significantly increase the susceptibility of weld solidification cracking of Alloy 709. This conclusion was supported by limited experimental data that showed poor weldability and considerable cracking for experimental Alloy 709 heats (< 20 wppm P) when welded with weld wires of high P levels (Yamamoto, 2014,), although optimizing and carefully control of the welding parameters could result in improved weld quality and pass the ASME Section IX qualification tests (Feng, et al., 2021, 2020, 2019).

A total of three Alloy 709 weld wires with different P levels (140 wppm, 30 wppm, and < 20 wppm) have been investigated so far. They were produced from three heats of Alloy 709 plates by wire drawing process: 140 wppm P from commercial Heat-1 (Heat 58776-4A), 30 wppm P from the commercial Heat-2 (Heat 529900), and < 20 wppm P from lab Heat 011367-08. Table 3 lists the chemical compositions of three wires. All three weld wires used in this welding research meet the specified NF709 chemical requirements.

Table 3. Chemical compositions of plates for fabrication of Alloy 709 weld wires (wt.%).

Alloy 709 weld wires	A709 wire-140wppm	A709 wire<20wppm	A709 wire-30wppm	ASME SA-213 UNS-S31025 Specification
	Heat number 58776-4A	Heat number 011367-08	Heat number 529900	
C	0.07	0.079	0.08	0.10 max
Cr	19.93	20.03	19.9	19.5–23.0
Co	0.02	<0.01	0.02	–
Ni	24.98	25.05	24.6	23.0–26.0
Mn	0.91	0.87	0.9	1.50 max
Mo	1.51	1.48	1.5	1.0–2.0
N	0.148	0.156	0.15	0.10–0.25
Si	0.44	0.28	0.39	1.00 max
P	**0.014**	**<0.002**	**0.003**	**0.030 max**
S	<.001	<0.0013	<0.001	0.030 max
Ti	0.04	<0.01	<0.01	0.20 max
Nb	0.26	0.28	0.17	0.10–0.40
Al	0.02	0.02	0.02	–
B	0.0045	0.003	0.004	0.002–0.010
Cu	0.06	<0.01	0.06	–
Fe	Balance	Balance	Balance	Balance

2.3 ALLOY 709 WELD GEOMETRY AND TEST SPECIMENS

Single V groove with 20° bevel was the geometry used for welding of the Commercial Heat-1 base metal plates which had nominal thickness of 1.125 in and. Double-V groove was used for the for welding of the Commercial Heat-2 base metal plates, which had nominal thickness of 2.05 in. They are shown in Figure 1.

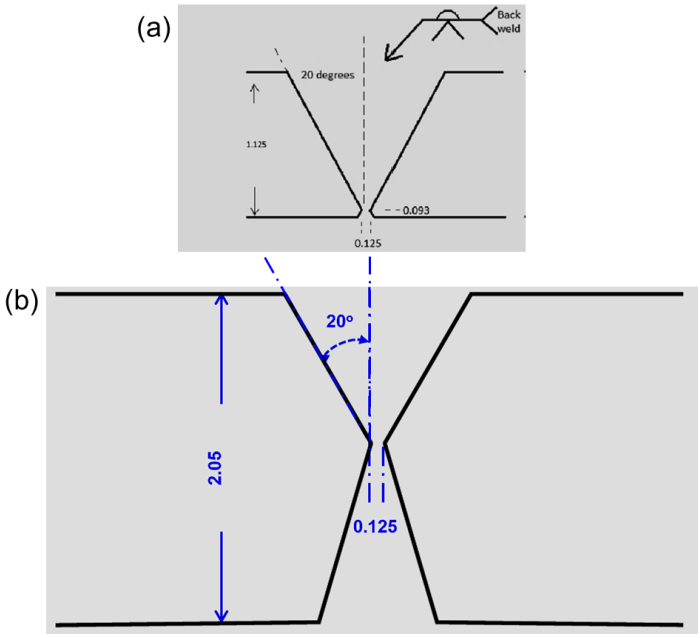

Figure 1. Single V-groove joint and double V preparation details used in the study.
Dimensions are in inches.

Room temperature cross-weld tensile tests are required per welding procedure qualifications requirements in ASME Section IX. The tensile specimen geometry and dimensions for Alloy 709 welds are shown in Figure 2. Two sets of tensile tests were performed on each weld for evaluation of the room temperature properties. For the welds with plate thickness of about 1-in, each set of the tensile tests include two specimens, whereas the thicker weld with ~2-in thickness had 4 tensile specimens each set. The centerline of the weldment is at the mid-length of the gage section, and the entire weld was within the reduced section of the tensile specimen.

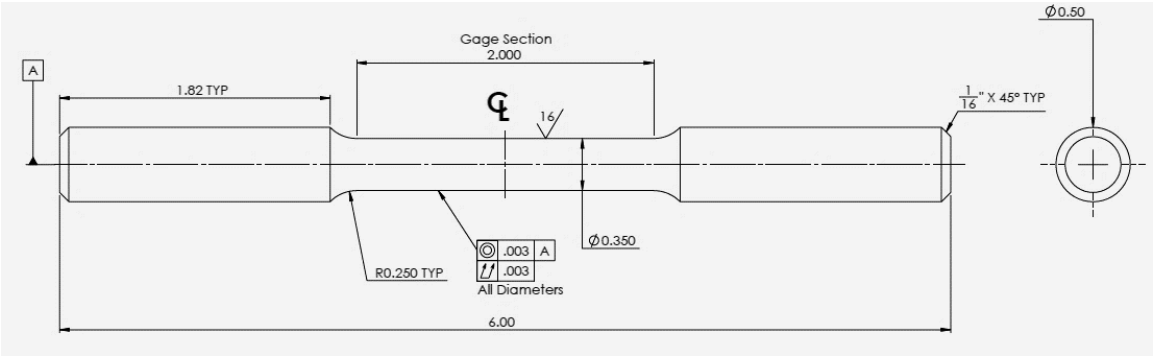

Figure 2. Room temperature cross-weld tensile specimen geometry.
Dimensions are in inches.

The location of the tensile specimens relative the weld zone is shown in Figure 5. The two sets of tensile specimens from the 1-in plate are (C1, R1) and (C2, R2) and the two sets of tensile specimens from the 2-in plate are (C1, R1, R3, C3) and (C2, R2, C4, R4). The "C" specimens are located at that "cap" of welds and the "R" specimens located at the root of the welds. The tensile test procedure followed ASTM E8 (ASTM, 2022).

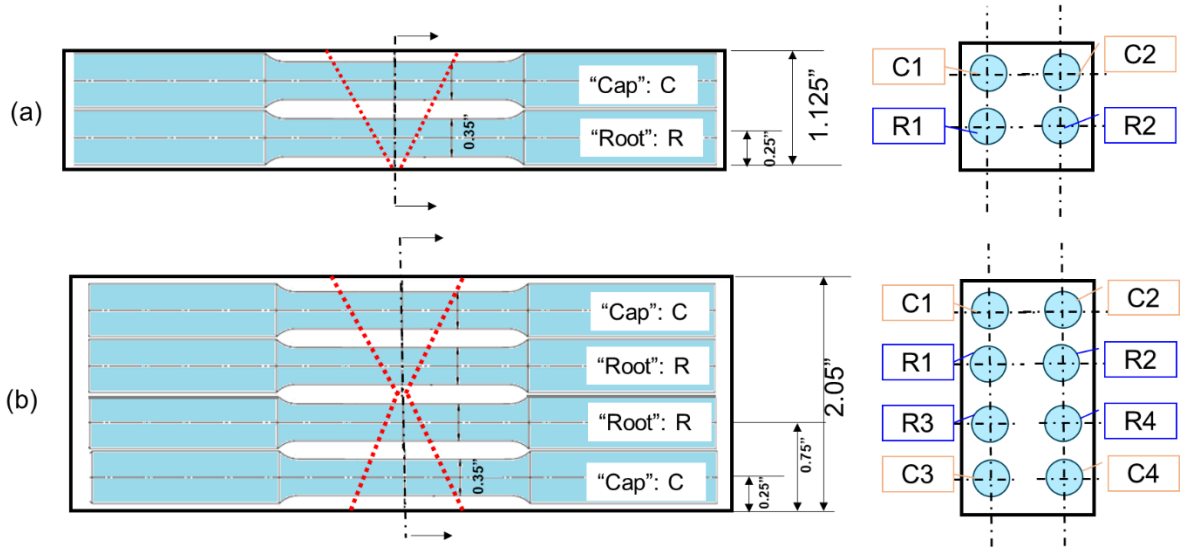

Figure 3. Schematics of the locations of the cross-weld weld tensile specimens

In support of Alloy 709 code qualification, cross-weld creep testing is also tasked under this welding research program. The weld creep specimen used the same geometry as the base metal creep specimen, shown in Figure 4.

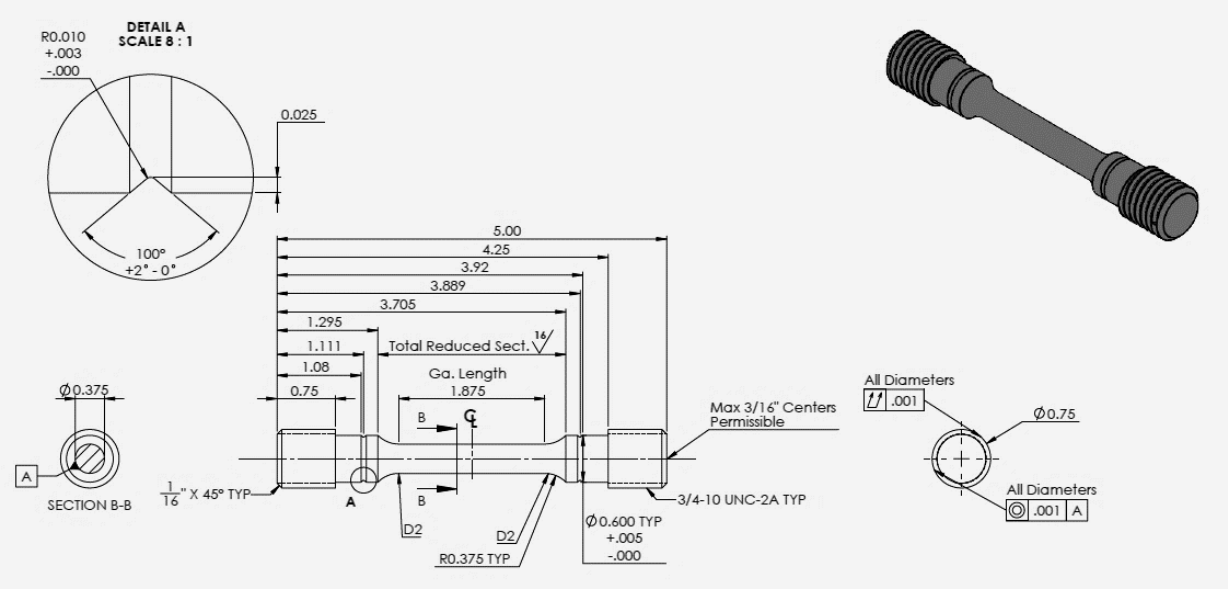

Figure 4. Alloy 709 cross-weld creep specimen geometry
Dimensions are in inches.

One cross-weld creep specimen was machined in the thickness direction of the 1-in plate welds and two from the 2-in plate weld, as shown in Figure 5. The cross-weld creep specimens are machined to allow the centerline of the weldment at the mid-length of the gage section, and the entire weld was within the reduced section of the tensile specimen.

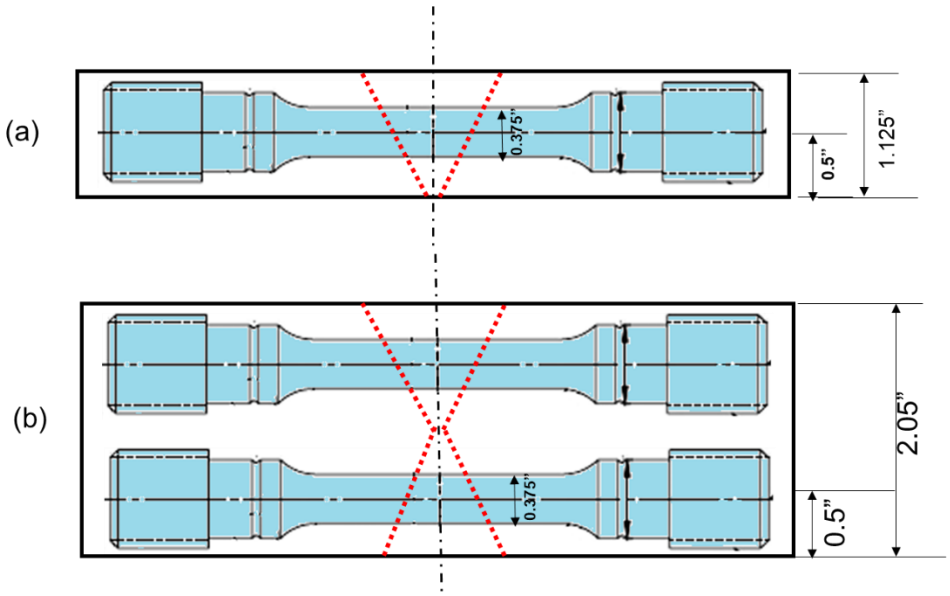

Figure 5. Schematics of the location of the cross-weld weld creep specimens.
Dimensions are in inches.

3. FABRICATION AND QUALIFICATION OF ALLOY 709 PRODUCTION WELDS

3.1 ALLOY 709 PRODUCTION WELDS

In support of Alloy 709 Code Case development, production welds were fabricated at ORNL to produce Code Case testing specimens. The welding procedure and parameters of the production welds are the same as what was developed for welding with low P weld wire (< 20 wppw P) (Feng, et al., 2019, 2020, 2021). Fabrication of the first production weld, W10, on the commercial Heat-1 plates was completed in FY 2021, and it is 15 inches in length. In this study, the same welding parameters were used to fabricate the second production weld on the commercial Heat-2 plates. Note that the commercial Heat-2 plate has a nominal thickness of 2.05 inches. The total length of this this second production weld is 27.5 inches.

The details of the two Alloy 709 production welds produced in support of the Code Case testing are summarized in Table 4. Photographs of the production welds are shown in Figure 6. X-ray inspection results were acceptable with no relevant indication of welding defects for both welds. Completion of the fabrication of this production weld allows creep rupture Code Case testing of the Stress Reduction Factors (SRF) required for the Alloy 709 Code Case data package.

Table 4. Alloy 709 production welds

Alloy 709 welds		Production weld-W10	Production weld-W11
Weld Wire	P Level (wppm)	< 20	< 20
	Heat No. of the supply material for weld wire	011367-08	011367-08
	Wire dia. (in)	0.035	0.035
Base Metal Plate		Commercial Heat 1 (Heat No. 58776)	Commercial Heat 2 (Heat No. 529900)
Base metal plate thickness (in)		1.12	2.05
Total weld length (in)		15	27.5
Weld joint geometry		20° single V	20° double V
ASME Sec. IX Weld Qualification	X-Ray	Pass	Pass
	Side Bend	Pass	Pass
	RT Tensile	Pass	Pass

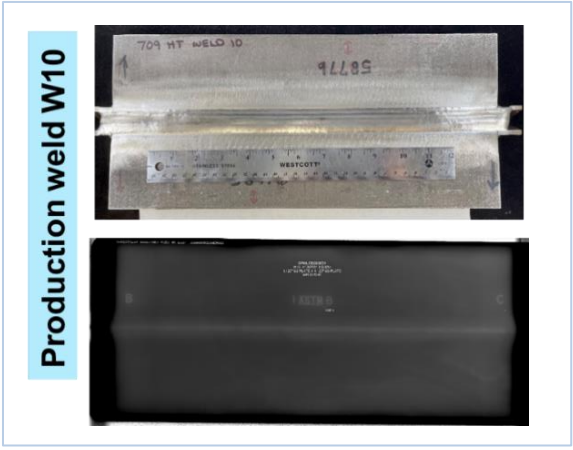

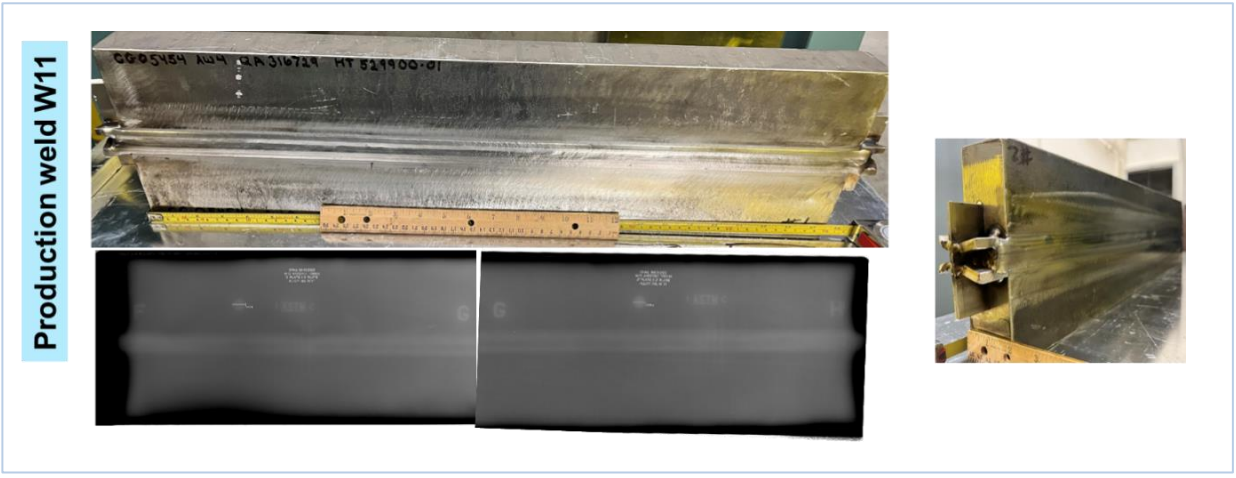

Figure 6. Photographs of the Alloy 709 production welds.

3.2 QUALIFICATION TESTS OF THE PRODUCTION WELDS

Four sets of room temperature side-bend weld qualification tests were performed on both production welds, W10 and W11. The side-bend specimens were 0.375-in in width and covered the entire thickness of the welds. Photographs of the side-bend specimens for both production welds after testing are shown in Figure 7. No cracks were identified after the side-bend testing for all specimens, and both production welds passed the side-bend testing.

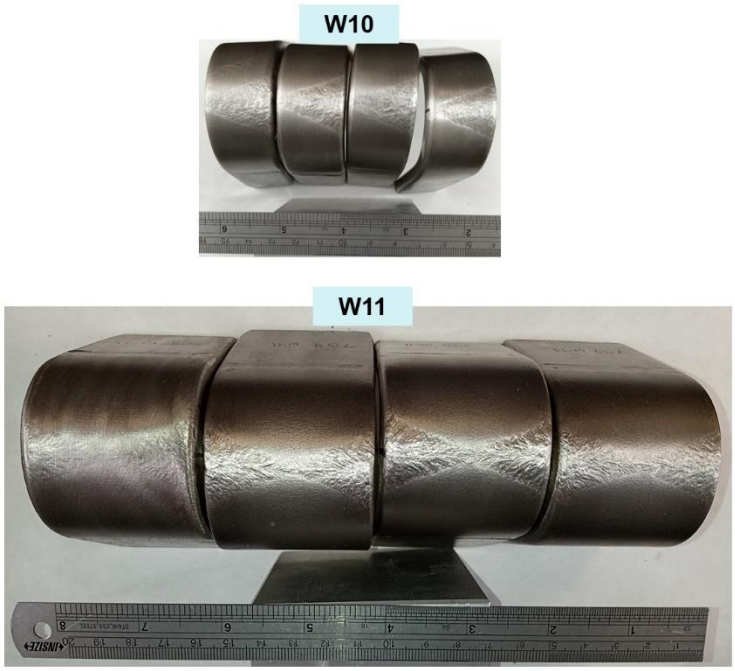

Figure 7. Photographs of the side-bend specimens of the production welds after testing

Two sets of room temperature cross-weld tensile tests were completed on the two production welds. The stress-strain curves for the four tensile tests on weld W10 are presented in Figure 8 and the tested tensile specimens are photographed in Figure 9, whereas the corresponding results for the eight tensile tests on weld W11 are in Figure 10 and Figure 11. The center of the weldment was marked with arrows in the photographs. The ultimate tensile strengths are summarized in Table 5.

All the tensile tests on both production welds failed in a ductile manner and the ultimate tensile strength values are above the ASME SA-213 UNS-S31025 specified 640 MPa minimum for base metal, hence both welds passed the ASME Section IX weld tensile qualification testing requirements.

Production weld W10 is stronger in tensile than weld 11. For both welds, the cap of the weld consistently showed slightly lower tensile strength than the root of the weld. All four tensile specimens from production weld W10 failed inside the weldment. The four tensile specimens from the cap of the weld W11 failed inside the weld, whereas the tensile specimens from the root of the weld W11 failed in the base metal.

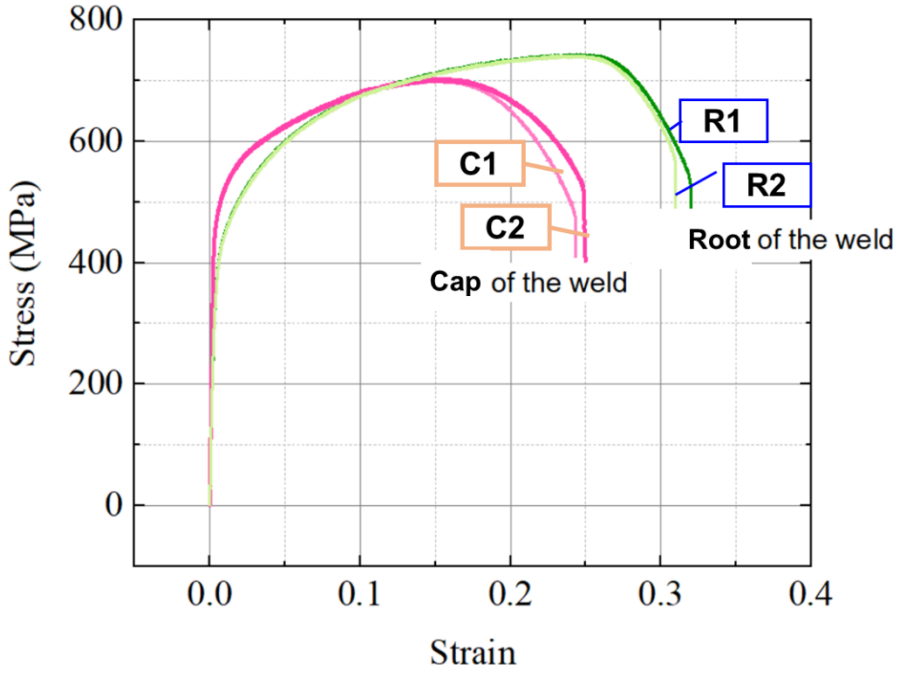

Figure 8. Room temperature cross-weld tensile results for production weld W10.

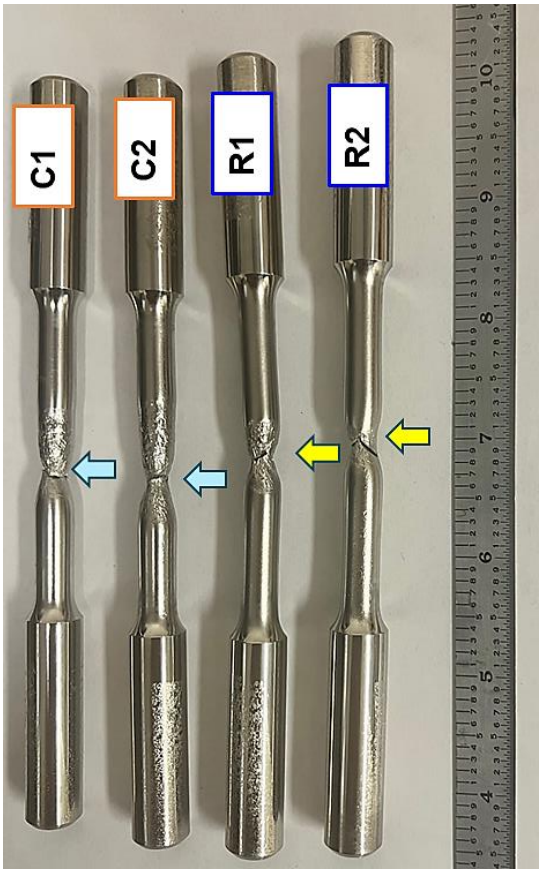

Figure 9. Photograph of the tested cross-weld tensile specimens from production weld W10

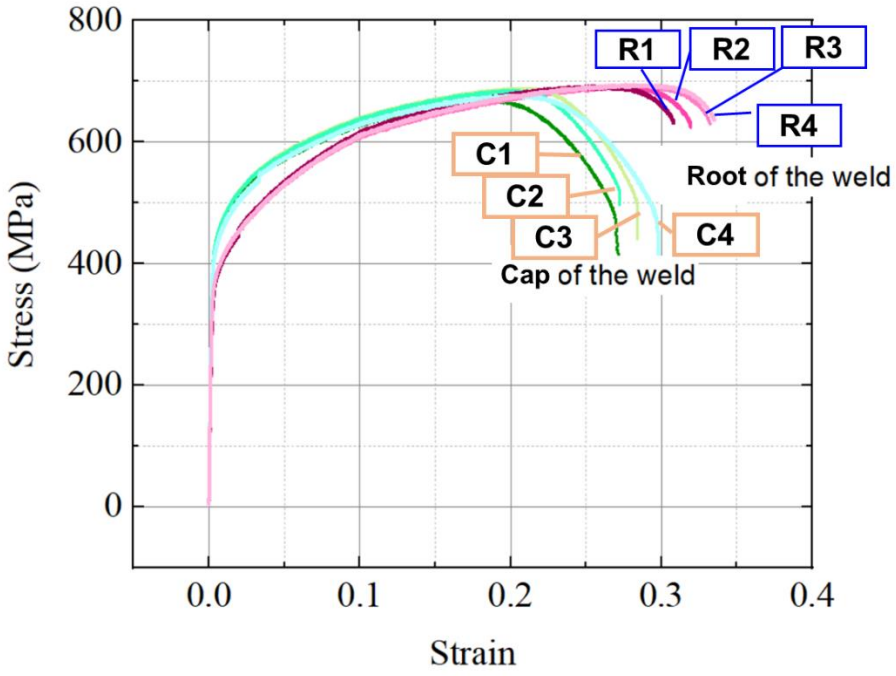

Figure 10. Room temperature cross-weld tensile results for production weld W11.

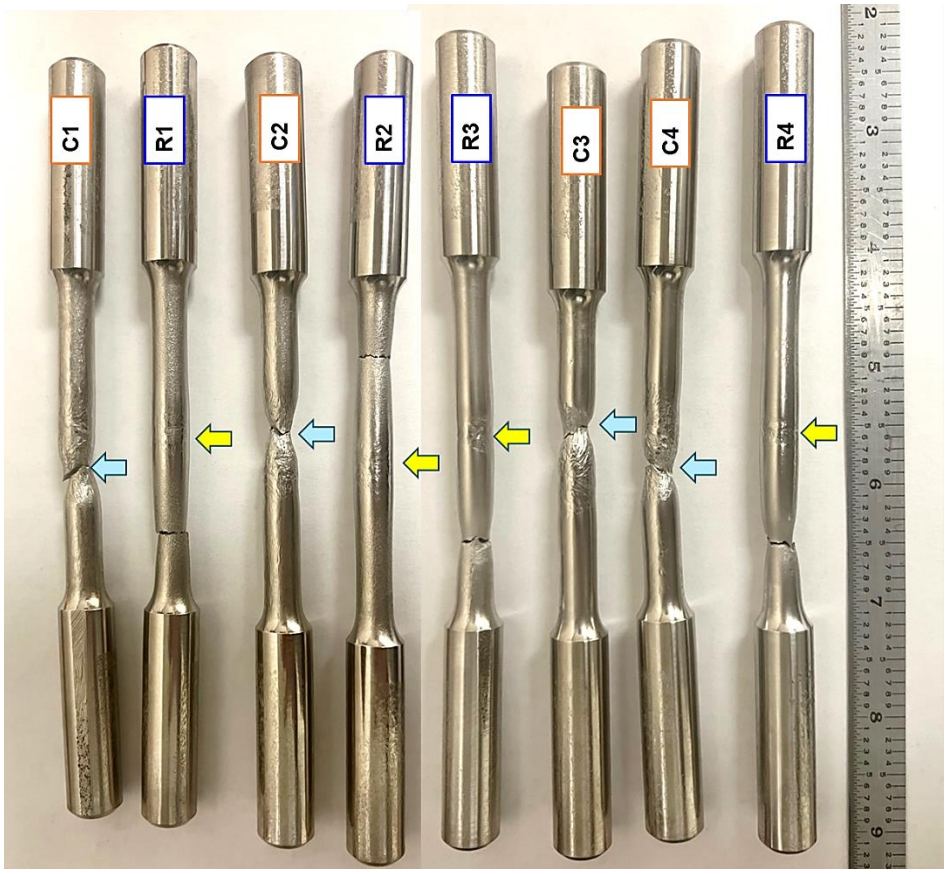

Figure 11. Photograph of the tested cross-weld tensile specimens from production weld W11

Table 5. Room temperature cross-weld tensile test results for the production welds

	Location of the tensile specimens	Tensile strength (MPa)
Production weld W10 cross-weld tensile tests	Cap of the weld C1	700.4
	Cap of the weld C2	702.9
	Root of the weld R1	742.7
	Root of the weld R2	740.7
Production weld W11 cross-weld tensile tests	Cap of the weld C1	668.3
	Cap of the weld C2	668.7
	Cap of the weld C3	668.7
	Cap of the weld C4	677.0
	Root of the weld R1	679.9
	Root of the weld R2	684.2
	Root of the weld R3	688.7
	Root of the weld R4	694.7

3.3 MICROSTRUCTURE CHARTERIZATION OF THE PRODUCTION WELDS

3.3.1 Microstructure characterization of the production weld W10

A metallurgical analysis was conducted to characterize the typical microstructures of the weld and its sub-regions. The optical images in Figure 12 shows the cross-section of the entire weld W10. No obvious weld defects or cracks were observed in the weld.

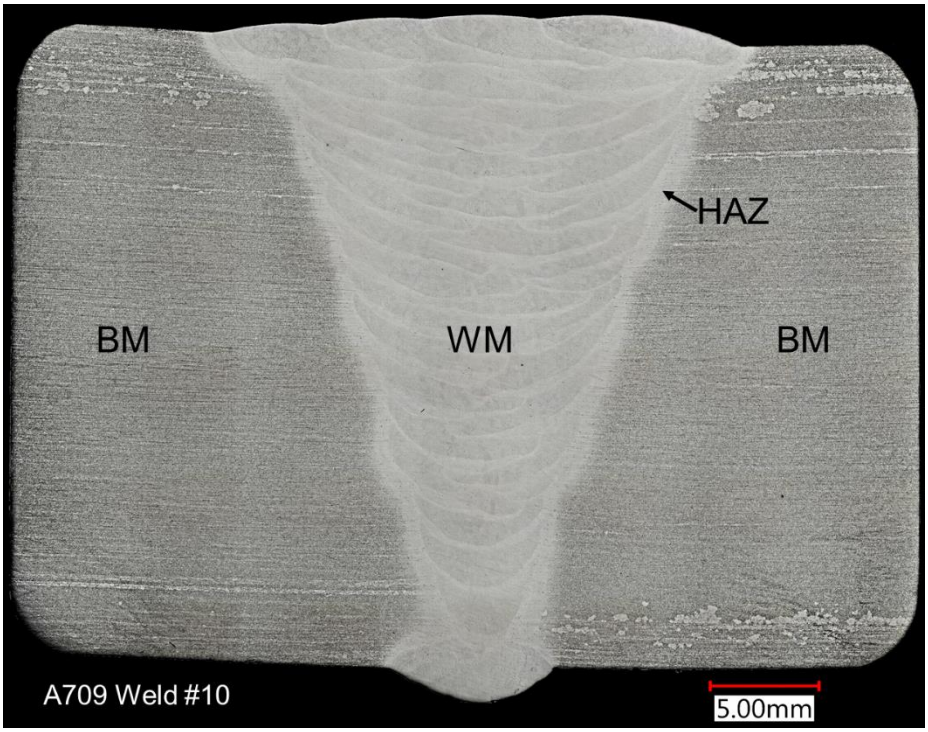

Figure 12. Optical image showing cross-section of the weld W10.
No obvious weld defects or cracks were observed.

Figure 13 presents the typical microstructure of the solidified weld metal without cracks. The higher-magnification image in Figure 13(b) shows the solidified dendritic microstructures with some small particles. Figure 14 shows the typical microstructure of heat affected zone (HAZ) near the fusion line (FL). Based on the image contrast, the HAZ adjacent the FL had experienced considerable microstructure changes in matrix grains and precipitates, comparing with the base metal. Large particles are still visible in the HAZ.

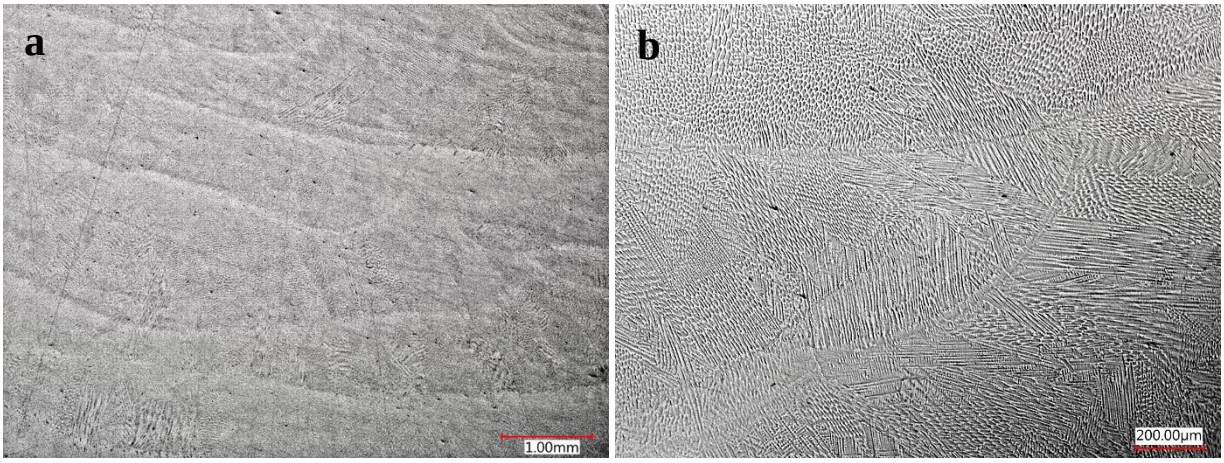

Figure 13. Optical images showing typical microstructure of solidified weld metal for W10

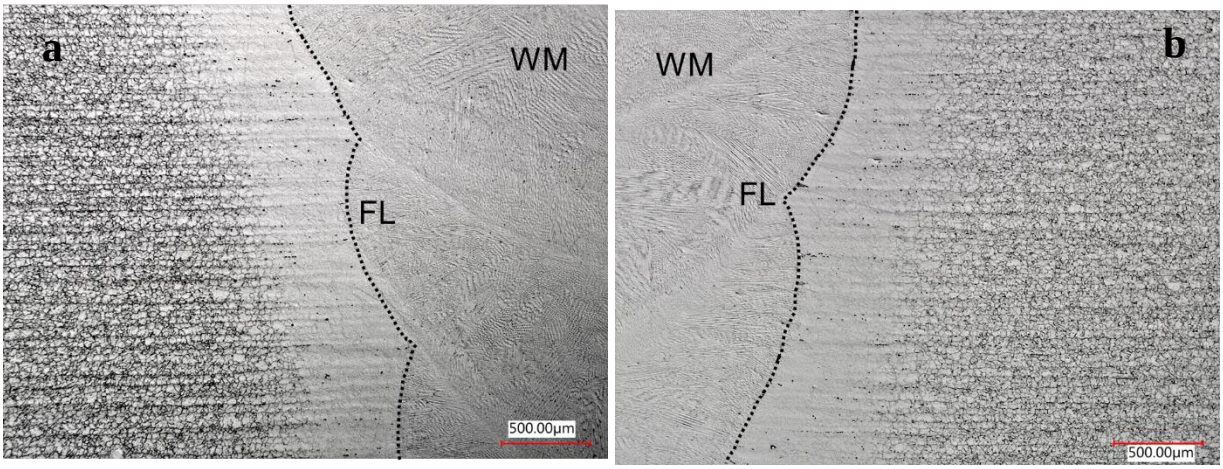

Figure 14. Optical images showing typical microstructure of HAZ near the fusion line (FL)of W10

3.3.2 Hardness measurements of the production weld W10

Figure 15 shows multiple microhardness line distributions across the cross-section of the weld along the plate thickness direction. There are some hardness variations (190-270 HV0.5) of the weld metal (WM) along the thickness direction. The WM in the root region has the highest hardness of 270 HV0.5 while the WM in the top cap region has the lowest hardness of 190 HV0.5. Noticeable hardness increase is also observed in the HAZ. The hardness in HAZ increased from ~200 HV0.5 in the BM to ~260 HV0.5 at the fusion line. High-resolution hardness mapping in Figure 16 revealed a high hardness band (250-260 HV0.5) with a total width of ~2.8 mm in the region from the fusion line. Figure 17 shows both large and fine particles near a typical hardness indent in the HAZ. No continuous precipitates are observed along the grain boundaries under optical microscopy. Meanwhile the high hardness band presents a soft-hard layered structure, which is likely related with the original microstructure of BM. It is noted that such

hardness variations in the HAZ and weld metal of Alloy 709 are consistent with those of the welds reported in previous research periods (Feng, et al., 2019, 2020, 2021).

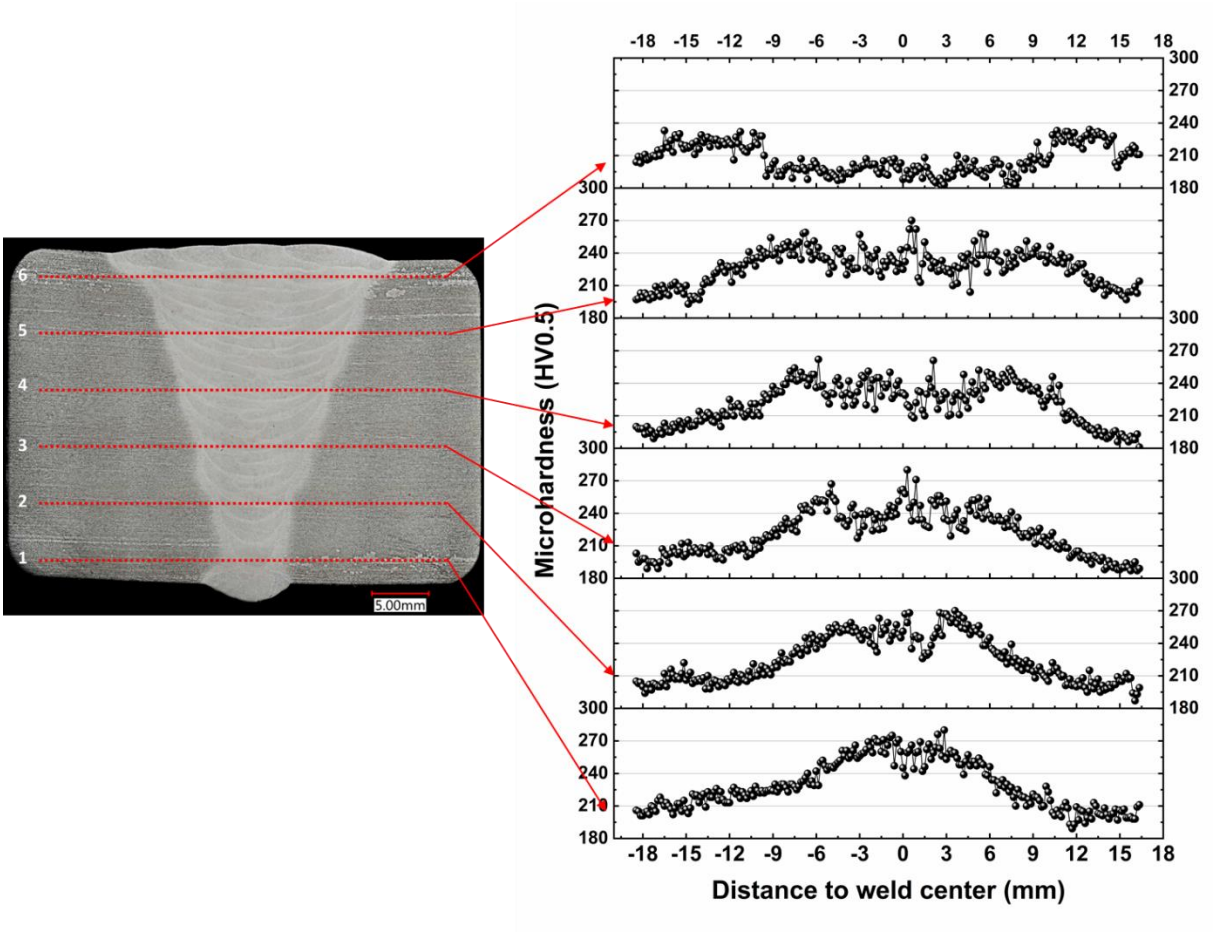

Figure 15. Micorhardness distributions across the cross-section of the weld W10

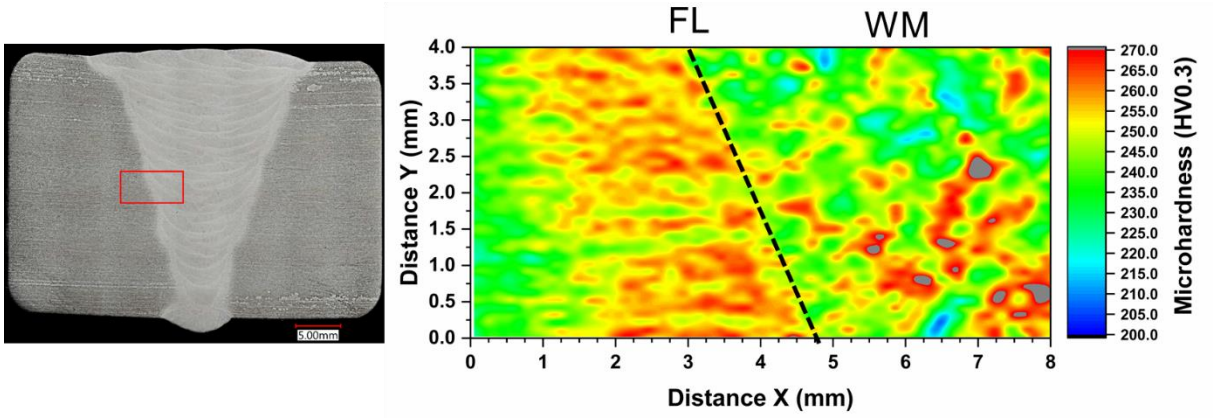

Figure 16. High-resolution micorhardness mapping aound the HAZ at mid-thickness of weld W10.

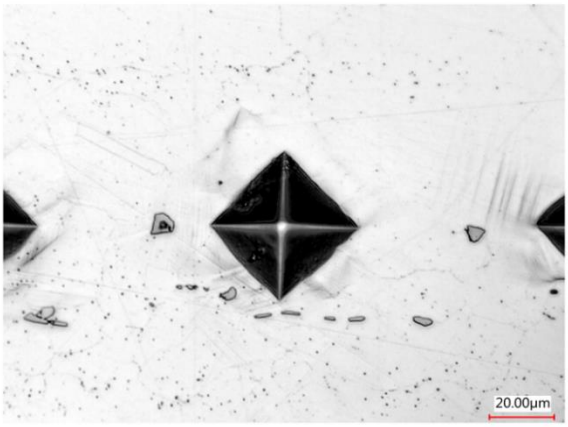

Figure 17. Optical image showing tyical hardness indent and particles in the HAZ

3.3.3 Microstructure characterization of the production weld W11

A metallurgical analysis was conducted to characterize the typical microstructures of the 2”-thick double-V groove production weld W11 and its sub-regions. The optical images in Figure 18 shows the cross-section of the entire weld W11. No obvious weld defects or cracks were observed in the weld.

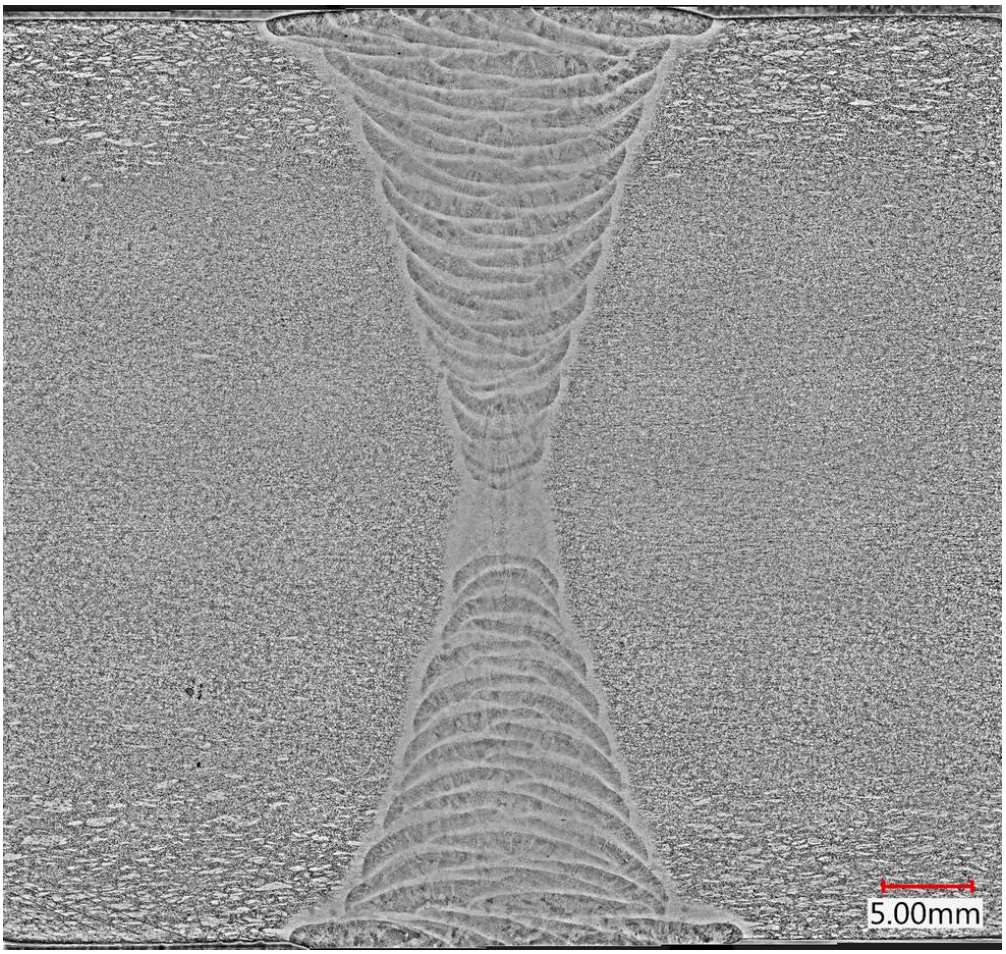

Figure 18. Optical image showing the cross-section of the 2”-thick production weld W11

The magnified images in Figure 19 show the solidified dendritic microstructure of the weld metal. No cracks were observed along the dendrite boundaries. Figure 20 shows the typical microstructure of the HAZ near the fusion line. The matrix grain coarsened in the HAZ adjacent to the fusion line. No cracks were observed along the fusion line or the grain boundaries in the coarse grained HAZ.

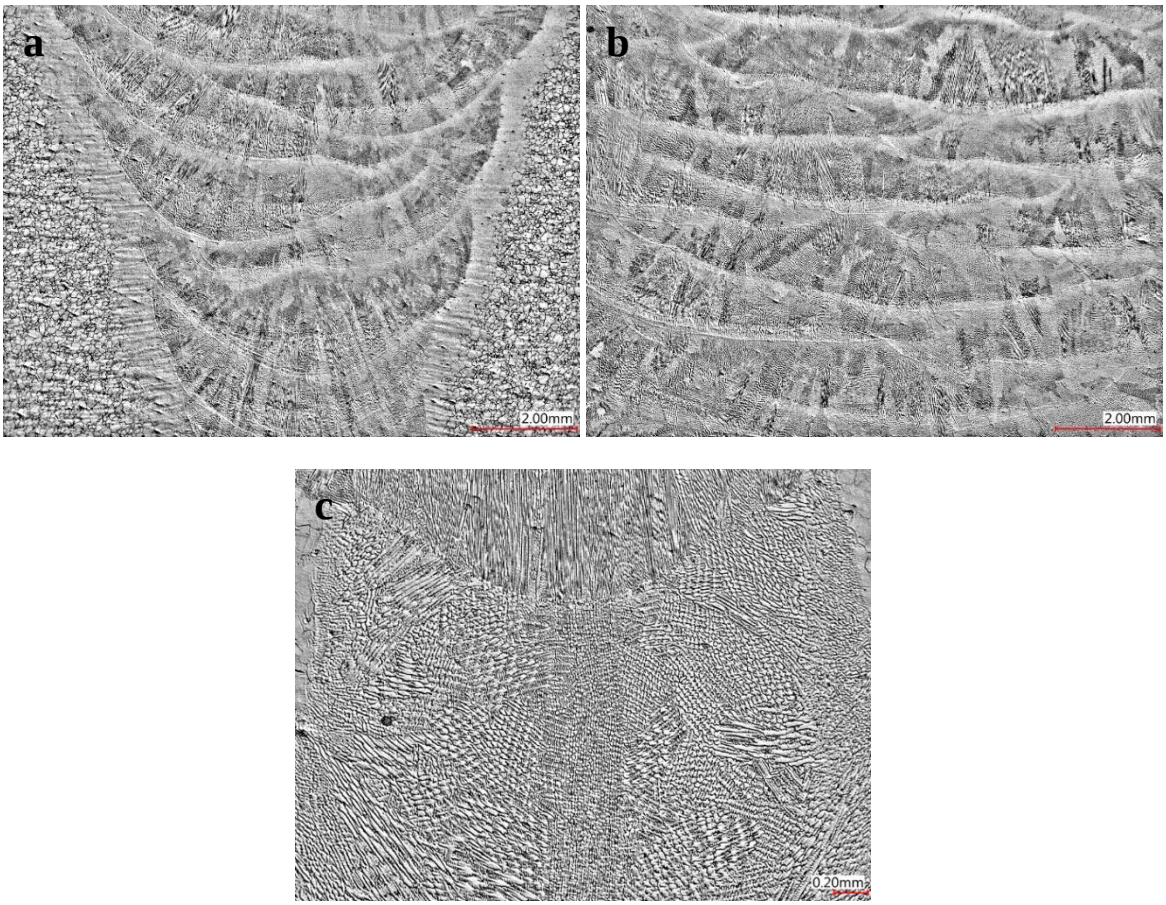

Figure 19. Optical images showing typical microstructure of solidified weld metal in W11.
No solidification cracking was observed

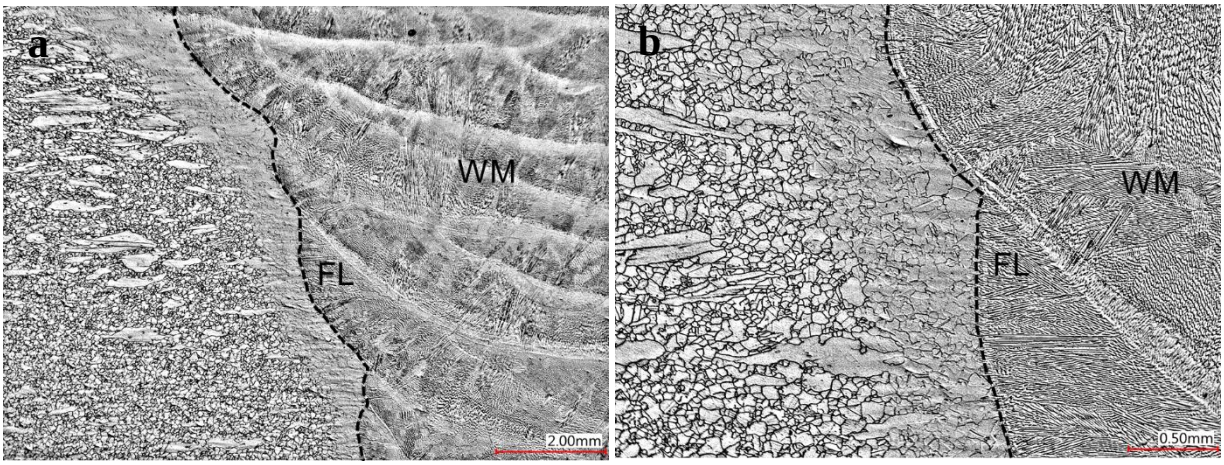

Figure 20. Optical images showing typical microstructure of HAZ near the fusion line (FL) of weld W11

4. RELAXING THE RESTRICTION OF P LEVEL IN ALLOY 709 WELD WIRE

4.1 ALLOY 709 WELD W12

In an effort of relaxing the restriction of the P content in the Alloy 709 weld wire, a new weld wire was fabricated from the commercial Heat-2 plates with 30 wppm of P (Heat No 529900). A test weld W12 was fabricated with this new weld wire on the first commercial heat plates with high P content of 140 wppm.

The weld W12 was inspected with X-ray and found acceptable per ASME Section IX with no relevant indications of welding flaws. A photograph of this weld is shown in Figure 21. Table 6 has summarized the critical information about this weld W12.

Figure 21. Photograph of W12 Weld.

Table 6. Alloy 709 Weld W12

Alloy 709 welds		Weld 12
Weld Wire	P Level (wppm)	30
	Heat No. of the supply material for weld wire	529900
	Wire dia. (in)	0.035
Base Metal Plate		Commercial heat-plate (Heat No 58776)
Base metal plate thickness (in)		1.12
Total weld length (in)		15
Weld joint geometry		20° single V
ASME Sec. IX Weld Qualification	X-Ray	Pass
	Side Bend	Pass
	RT Tensile	Pass

Weld 12 was further evaluated with side bending tests and tensile tests at room temperature. The results from four duplicate side bend tests showed no indications of any cracks in the weldment, as shown in Figure 22. Two sets of cross-weld tensile test specimens were machined from Weld W12. Each set of the tensile tests had one specimen out of the cap of the weld and one out of the root of the weld. The room temperature tensile stress-strain curves are plotted in Figure 23. The tensile strengths of the four test specimens are summarized in Table 7. The tensile strengths of all four specimens were above the minimum ASME code required base metal tensile strength of 640 MPa. For both sets of the tensile tests, the root of the weld consistently showed higher tensile strength than the cap of the weld.

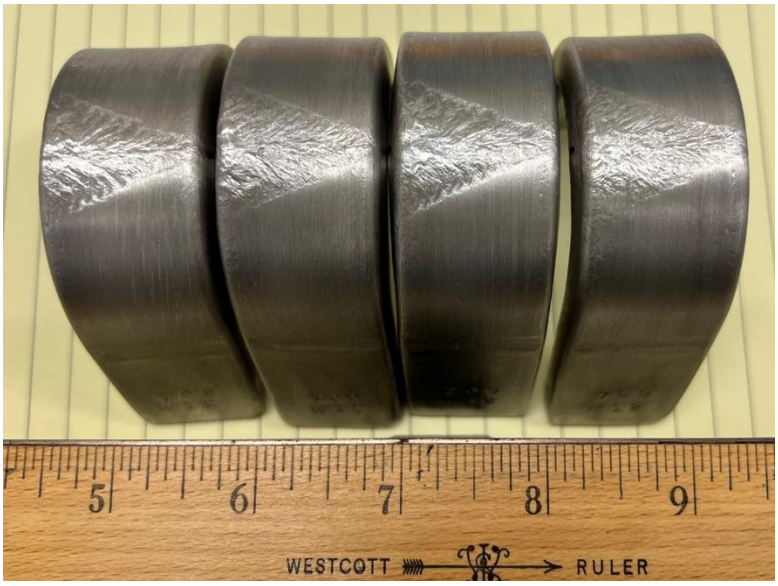

Figure 22. Photographs of the side-bend specimens after testing (W12)

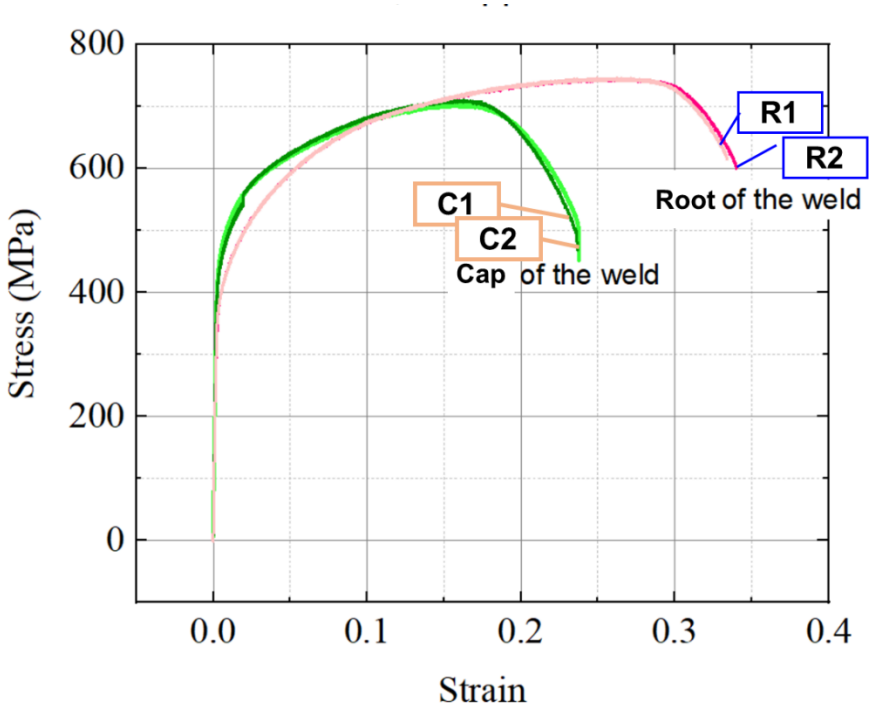

Figure 23. Room temperature cross-weld tensile results for Alloy 709 weld W12.

Table 7. Room temperature cross-weld tensile results for Weld W12

Location of the tensile specimens	Tensile strength, (MPa)
Cap of the weld 1	700.4
Cap of the weld 2	702.8
Root of the weld 1	740.8
Root of the weld 2	742.7

A photograph of the specimens after tensile tests is shown Figure 24. The center of the weldment was marked with an arrow. Both tensile specimens from the root of the weld failed in the base metal, i.e., outside the entire weldment. The failure location of tensile specimens from the cap of weld was inside the weldment. All four tensile specimens showed ductile failure mode.

As such, weld W12 passed the ASME Section IX weld quality requirement test. This weld passed all weld qualification tests without issues. This study provides confidence to take action in further relaxing the P content in future work.

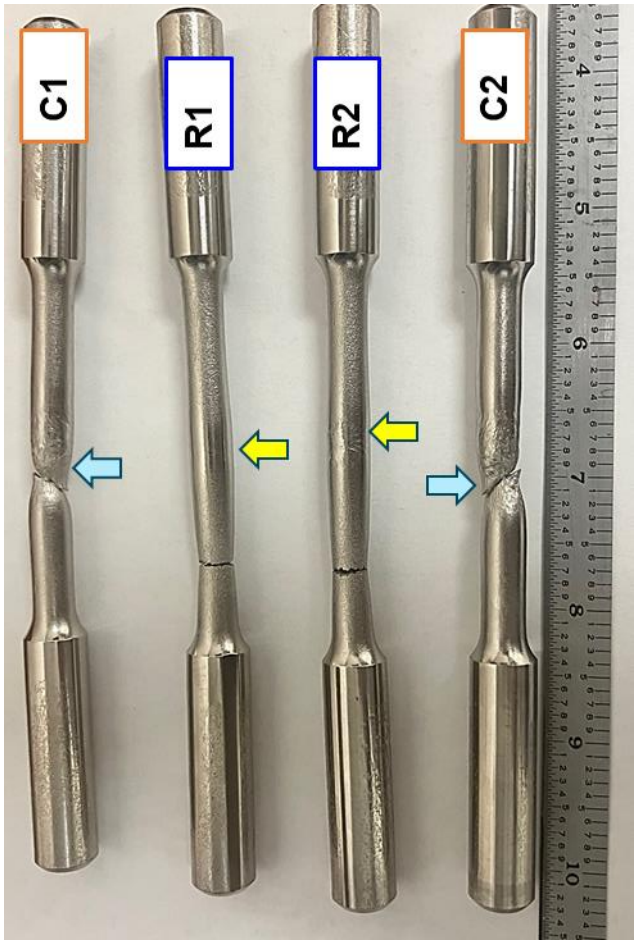

Figure 24. Photograph of the tested cross-weld tensile specimens from production weld W12

4.2 MICROSTRUCTURE CHARACTERIZATION WELD W12

A metallurgical analysis was conducted to characterize the typical microstructures of the weld (W12) and its sub-regions. The optical images in Figure 25 shows the cross-section of the entire W12 weld. A porosity was observed in the cap region of the weld metal, but no cracks were observed in the weld. The magnified images in Figure 26 and Figure 27 show the typical dendritic microstructure of the weld metal, which confirms no minor cracks were observed along the dendrite boundaries. Figure 28 shows the typical microstructure of the HAZ near the fusion line. No cracks were observed along the fusion line or the grain boundaries in the coarse grained HAZ. Dissolution of precipitates was observed in the coarsened grains. Some large particles and remaining precipitates along grain boundaries are still visible.

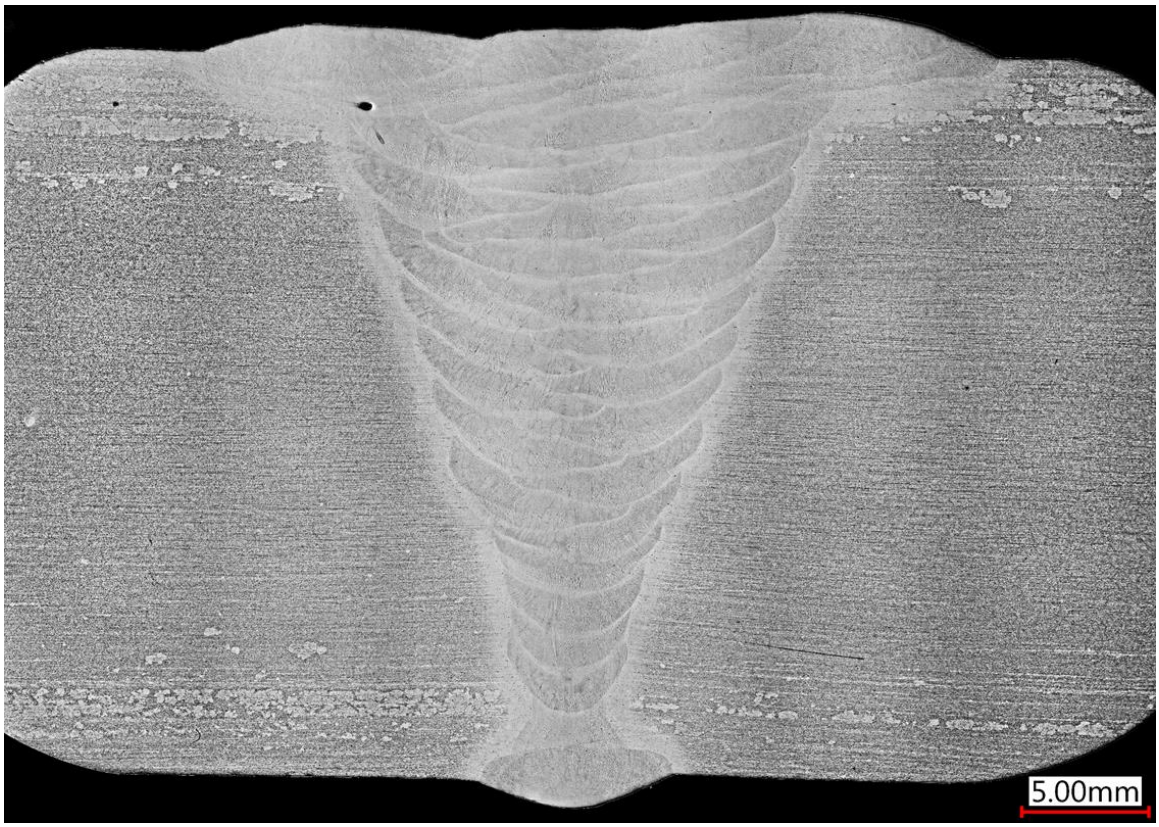

Figure 25. Optical image showing the cross-section of the weld (W12).
One porosity is observed on the cap region, but no cracks or other defects.

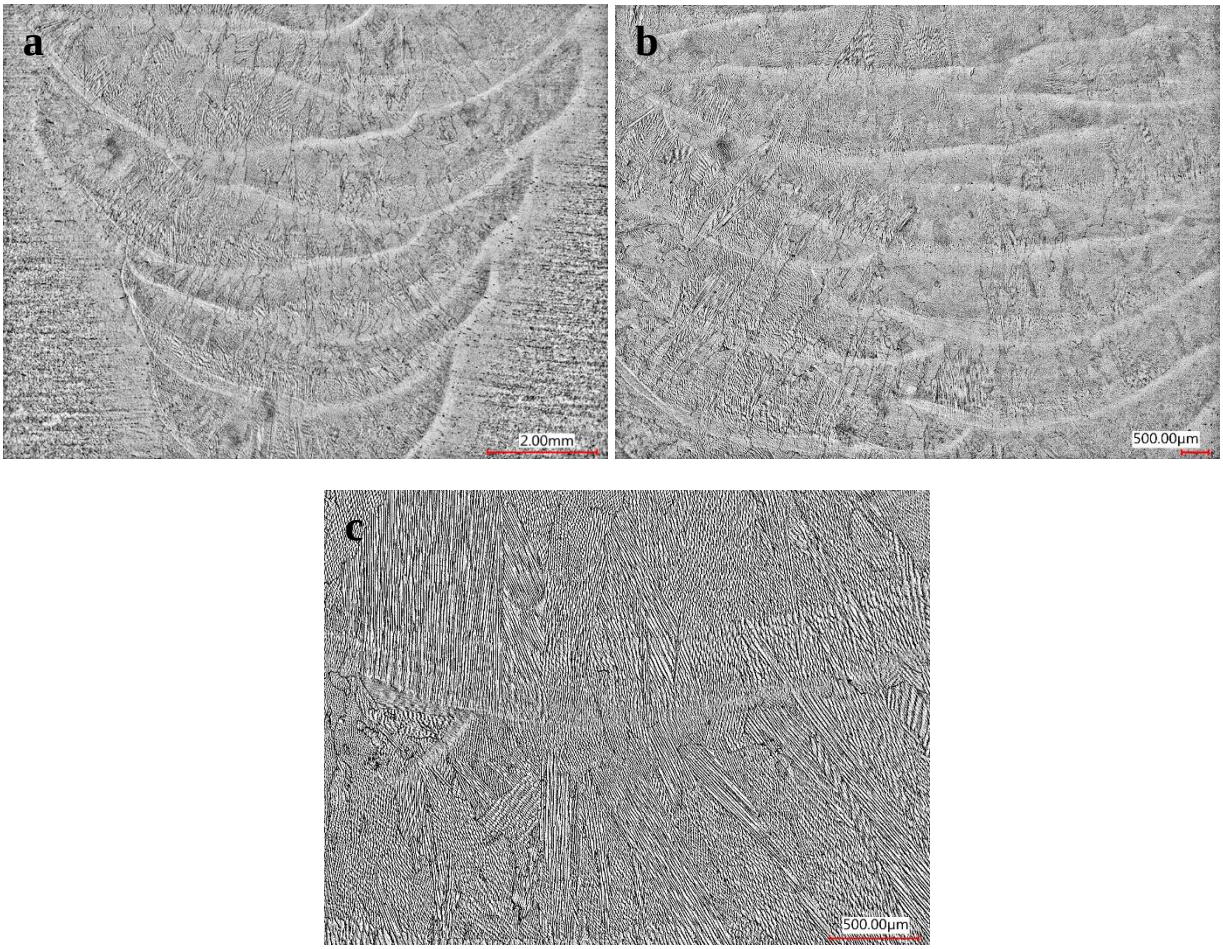

Figure 26. Optical images showing typical microstructure of solidified weld metal of W12.
No solidification cracking was observed.

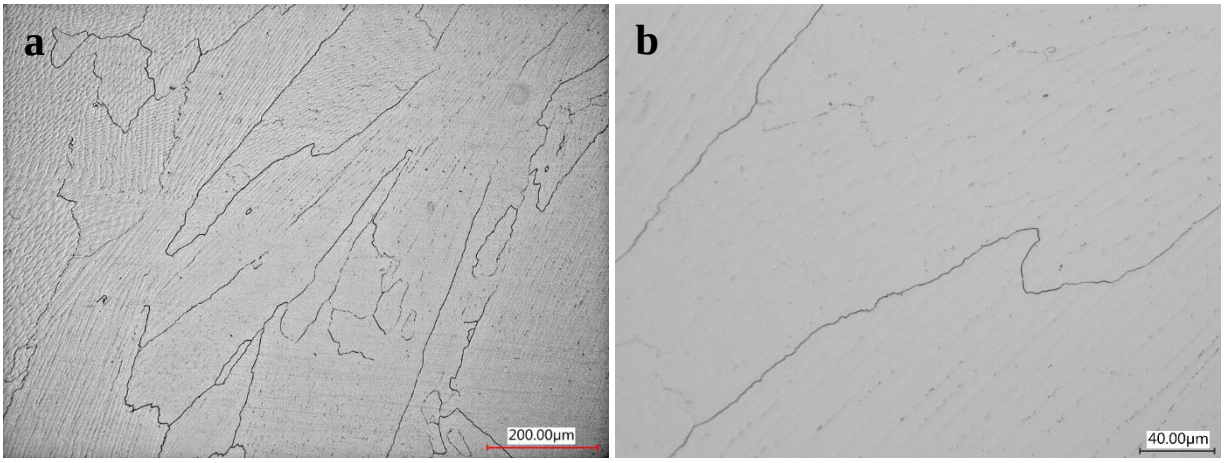

Figure 27. High-magnification optical images showing typical dendrite boundaries in the solidified weld metal of weld W12

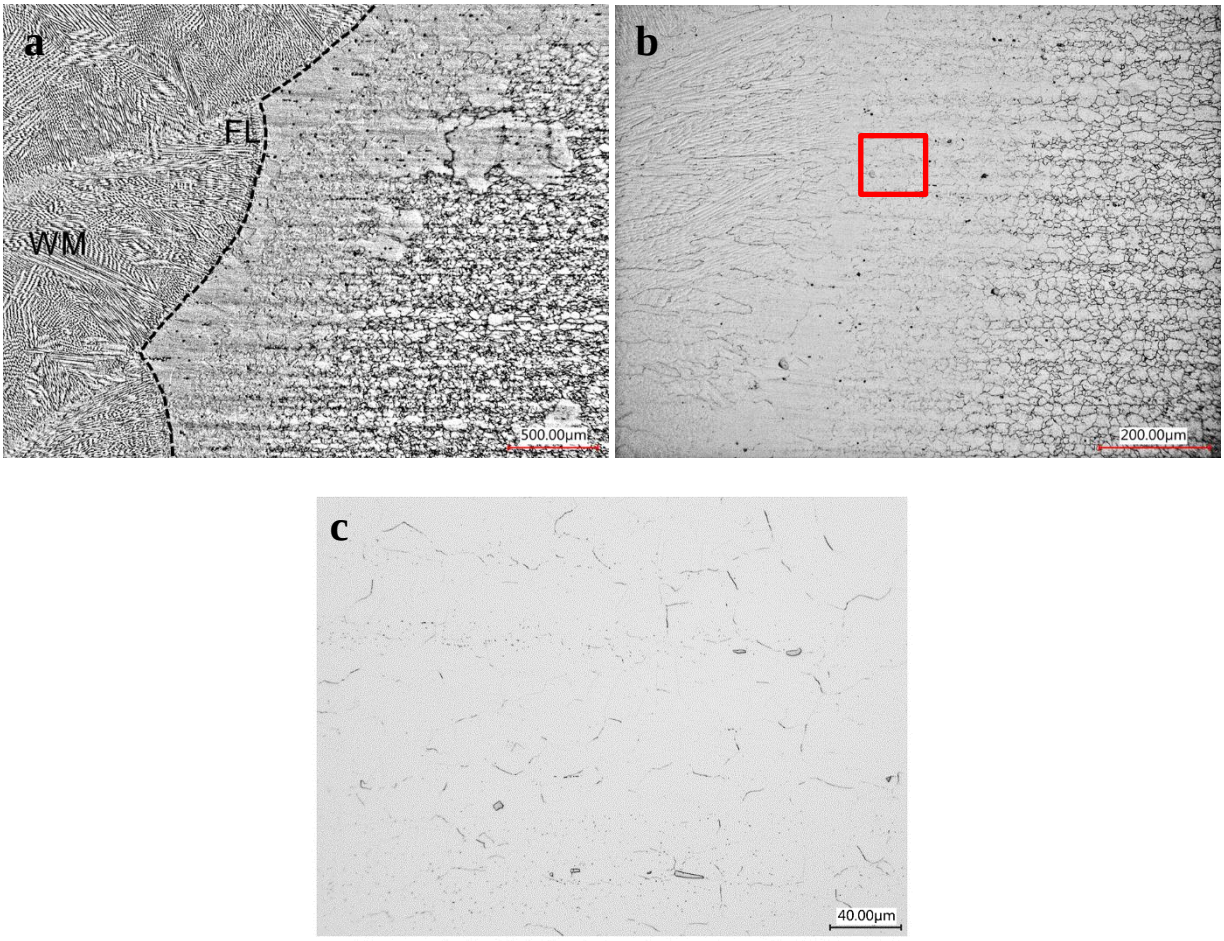

Figure 28. Optical images showing typical microstructure of HAZ near the fusion line (FL) of weld W12

5. PRELIMINARY CREEP TEST ON ALLOY 709 WELDS

Creep testing of the Alloy 709 welds continued on the test welds that passed the ASME Section IX qualification tests. Table 8 lists the creep testing parameters and the updated status of these preliminary creep tests on these welds. In this table, the weld identification numbers are consistent with the previous report in Feng et al. (2019, 2020, 2021). The results from the preliminary creep tests are used to develop the creep testing matrix for the more comprehensive creep testing on Alloy 709 weds in support of the development of the Alloy 709 Code Case data package.

For comparison purposes, the Larson-Miller relationship was used to compare all the available creep rupture results on the Alloy 709 welds with the rupture data generated on the two commercial heats of Alloy 709 base metal in precipitation treatment condition (PT condition) shown in Sham et al., 2022. The results are presented in Figure 29. In this plot, the Larson-Miller parameter (LMP) was based on Eq. (1):

$$LMP = (T + 273.15) * (16.6958 + \log t_r), \quad (1)$$

where T is temperature in degrees Celsius and t_r is rupture life in hours, and C is a constant.

This preliminary analysis indicates that the commercial heat 2-PT condition has slightly higher creep strength than the commercial heat-1-PT condition.

Table 8. Preliminary creep testing results of Alloy 709 welds

ID	Weld wire and base metal plates	Test number	Temp (ºC)	Stress (MPa)	Rupture time, (hr)
W2	**Weld wire heat#:** 011367-08 with P < 20 wppm; **Base meatal heat#:** 58776-3R with P content of 140 wppm	34276*	600	330	602.7
		34325*	600	330	378
		34455*	600	330	353
		34456	925	27	342
		34458	775	80	2300
W5	**Weld wire heat#:** 58776-4A with P content of 140 wppm; **Base meatal heat#:** 58776-3R with P content of 140 wppm	38440*	600	330	6.5
		38439	650	175	5,092.2
		38468	625	175	15940
		38467	650	150	15254.4
		38469	775	80	2464.5
W6	**Weld wire heat#:** 011367-08 with P< 20 wppm; **Base meatal heat#:** 58776-3RB with P content of 140 wppm**;** heat treated at 775 °C for 10 h	40014	750	100	2336
		40017	800	50	6055.7
		40980	800	35	Ongoing
		41185	725	75	Ongoing
		41186	700	90	Ongoing

Note: *These tests are excluded for creep strength evaluation due to the large loading strain beyond yield.

From the limited preliminary creep rupture data on weld W2, W5 and W6 and the comparisons with the base metal, the rupture life of Alloy 709 cross-welds continued to show little or no reduction in their creep strength. It is noted that tests at high stress of 330MPa at 600℃ are omitted in this analysis due to the large loading strain beyond the yield.

The creep testing matrix for the production weld is being developed, and the results will be used to establish the stress rupture factors for Alloy 709. The creep rupture Code Case testing of Alloy 709 welds will continue and testing of the production weld W10 and W11 will be initiated in FY 2023.

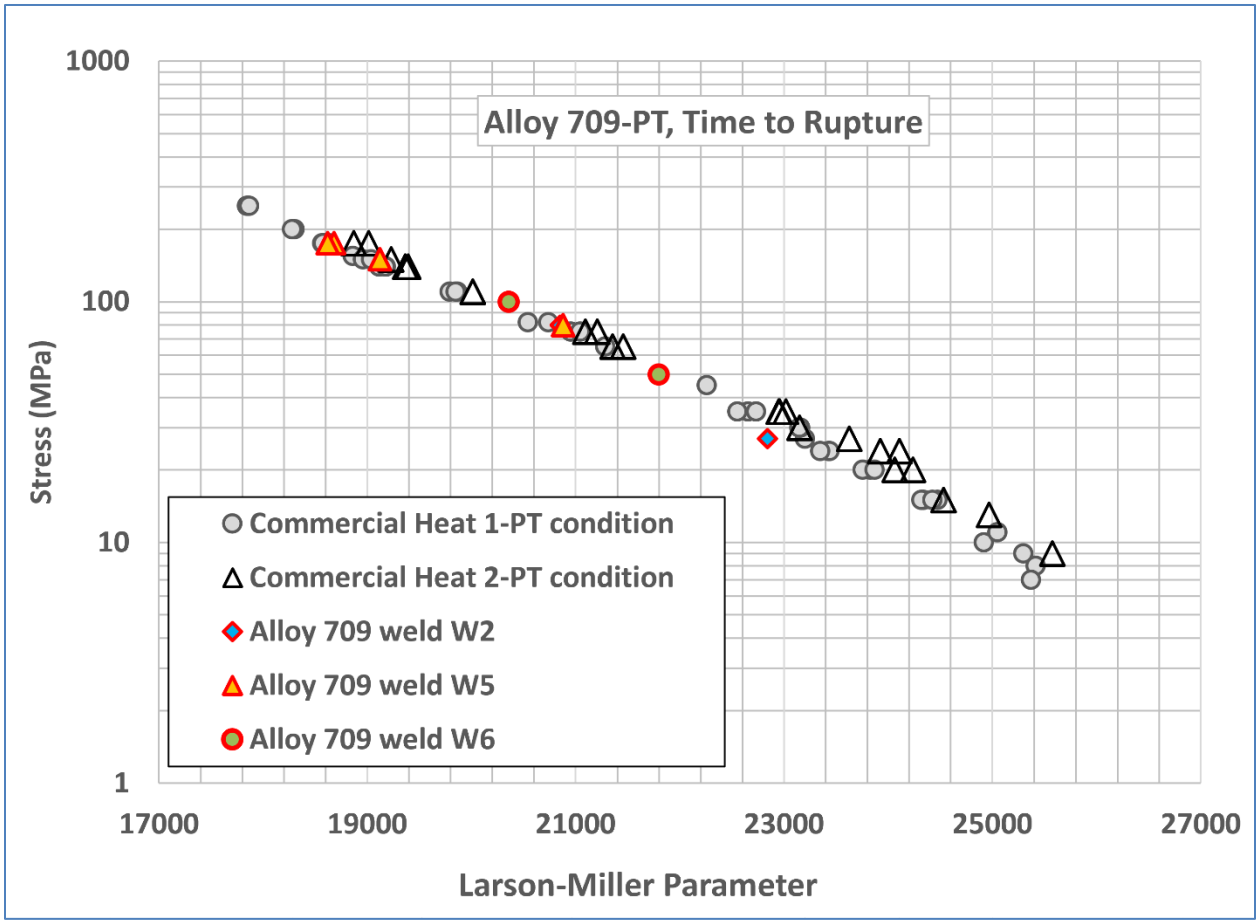

Figure 29 Comparison of creep rupture testing results of Alloy 709 welds and base metal in PT condition.

6. DEVELOPMENT OF CIRCULAR PATCH WELDABILITY TESTS FOR ASSESSING THE EFFECT OF P LEVEL ON WELD SOLIDIFICATION CRACKING

The circular patch weldability test is widely used for evaluating the solidification cracking susceptibility of stainless steels and nickel-based superalloys. It was adopted in this work to evaluate the effect of P level on solidification cracking susceptibility of Alloy 709. In FY 2022, we completed the development of experiment setup and welding/testing procedure using stainless steel 304L plate as the surrogate materials, due to the limited availability of Alloy 709 material. Figure 30 shows the circular patch test setup built at ORNL, specifically designed for testing the Alloy 709 filler metal with different P contents. The test system included a tungsten inert gas (TIG) welding torch, a wire feeder, weld camera, fixture plate, and test plate. The camera image on the right shows a typical example of solidification cracking in the weld metal right after the weld pool cooled and solidified.

The welding procedure and parameters were developed to ensure complete fill-up of the testing groove with Alloy 709 filler metal under different welding speed and heat input conditions. This was necessary to properly compare and evaluate the cracking susceptibility under different P levels.

Figure 31 show a typical example of the centerline solidification cracking after circular patch test using the low P Alloy 709 weld wire (P less than 20 wppm) on a 304L plate. Figure 32 shows cross-section

view of the centerline solidification cracking. The crack formed right in the center of the weld bead, which is the typical feature of solidification cracking. The solidification crack went through the specimen with a full penetration while the crack only propagated in the weld metal in the specimen without a full penetration.

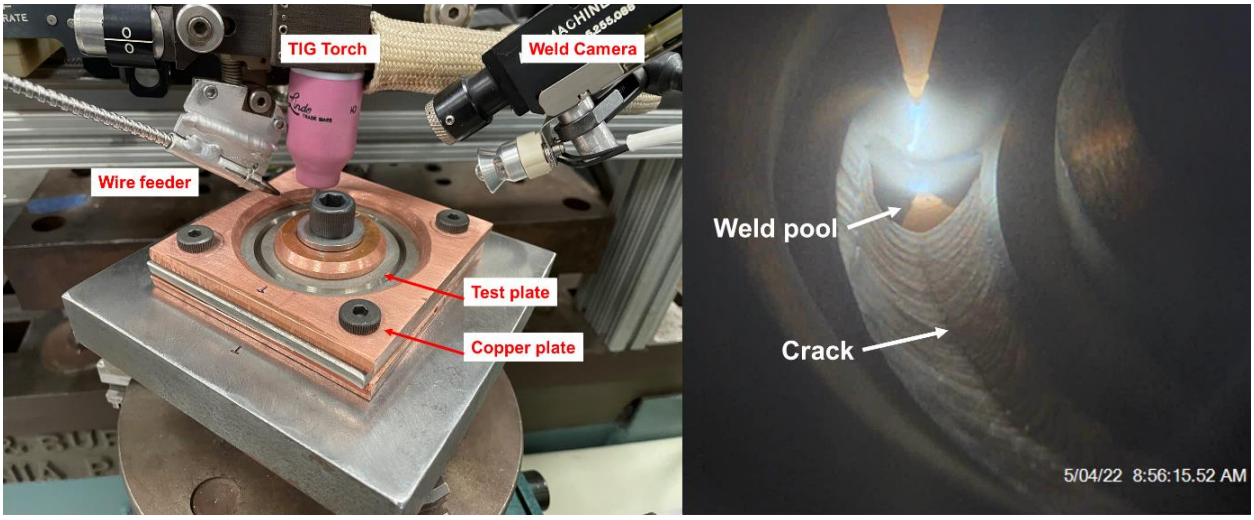

Figure 30.Circular patch test setup built at ORNL. The camera image on right shows centerline solidification cracking occurred during welding.

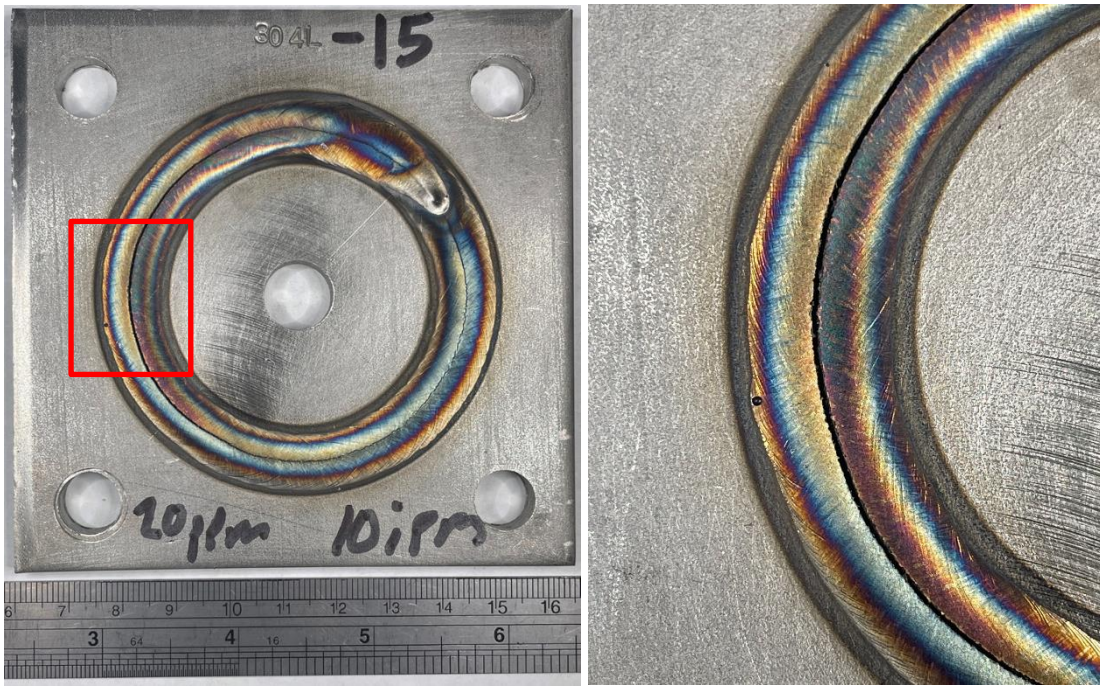

Figure 31. An example of the centerline solidification cracking after circular patch test using the Alloy 709 weld wire with <20 wppm-P on a 304L plate.

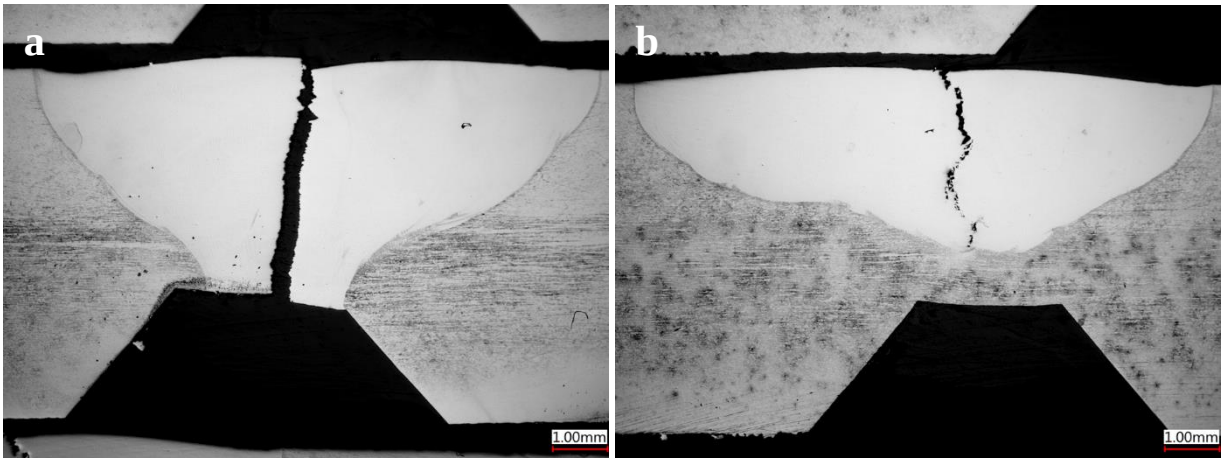

Figure 32. Cross-section view of the centerline solidification cracking after circular patch test test using the Alloy 709 weld wire with <20 wppm-P on a 304L plate.

Table 9 summarized all trials of the circular patch tests on 304 steel plates and 308 steel plates. Three 709 weld wires with a P level of <20 wppm, 30 wppm, and 140 wppm were used for these tests. The welding parameters, including heat input, travel speed, and wire feed speed, were optimized to differentiate the solidification cracking susceptibility of three wires

Table 9. Summary of the circular patch tests with 304L and 310 steel plates.

WELD#	ALLOY 709 WELD WIRE	BASE METAL	VOLTS	AMPS	RPM Groove= 2.375 Dia.	TRAVEL SPEED (imp) Groove= 2.375 Dia.	HEAT INPUT (JOULES PER INCH) (VOLTS*AMPS*60) /TRAVEL SPEED imps	WIRE FEED SPEED (ipm)	SOLIDIFICATION CRACKING	CRACK ANGLE (°)
050222-304-709-140PPM-1	140 wppm P Ht#58776-4	304L	11.2	145	0.67	5	19488	130	NO	
050222-304-709-140PPM-2			11.2	145	0.67	5	19488	120	NO	
050222-304-709-140PPM-3			11.2	145	0.67	5	19488	110	NO	
050422-304-709-140PPM-4			11	150	0.94	7	14143	50	YES	360
050422-304-709-140PPM-5			11	150	1.34	10	9900	50	YES	330
050422-304-709-140PPM-6			11	90	0.94	7	8486	50	N/A	
050422-304-709-140PPM-7			10	110	0.94	7	9429	28	YES	134+20
050222-310-709-140PPM-1		310	11.2	145	0.67	5	19488	110	NO	
050222-310-709-140PPM-2			11	150	0.67	5	19800	100	NO	
050322-310-709-140PPM-3			11	150	0.67	5	19800	80	NO	
050322-310-709-140PPM-4			11	150	0.67	5	19800	60	NO	
050422-310-709-140PPM-5			11	150	0.94	7	14143	50	NO	
050422-310-709-140PPM-6			11	150	1.34	10	9900	50	NO	
050422-310-709-140PPM-7			10	110	0.94	7	9429	28	NO	
072022-304-709-140ppm-8		304L	10.5	285	1.34	10	17955	195	YES	291
072022-304-709-140ppm-9			10	210	0.94	7	18000	140	YES	124
072022-304-709-140ppm-10			10	150	0.67	5	18000	95	No	
072622-304-709-140ppm-11 single V		304L	10	150	0.67	5	18000	105	NO	
072622-304-709-140ppm-12 single V			10	210	0.94	7	18000	140	NO	
072622-304-709-140ppm-13 single V			10.5	285	1.34	10	17955	200	NO	
080922-304-709-20ppm-14	< 20 wppm P Ht#011367-08	304L	10	210	0.94	7	18000	140	NO	
080922-304-709-20ppm-15			10.5	285	1.34	10	17955	195	YES	360
082222-304-709-40ppm-16	30 wppm P Ht#529900	304L	10.5	285	1.34	10	17955	195	YES	360
082222-304-709-40ppm-17			10	210	0.94	7	18000	140	YES	30

Figure 33 shows the solidification crack length increased with the travel speed and the P level. No cracking occurred when the travel speed is low (5 inch per minute, ipm) while all specimens cracked with a high travel speed (10 ipm). At a travel speed of 7 ipm, the effect of P level exhibits an obvious effect on the solidification cracking. Figure 34 shows the specimens welded with a travel speed of 7 ipm. No cracking occurred in the specimen with a low P wire (20 wppm-P). A 30° crack was observed in the specimen welded with a 30 wppm-P wire. The specimen welded with a 140 wppm-P wire cracked into 124°. These optimized weld parameters will be used for circular patch tests on the Alloy 709 plate.

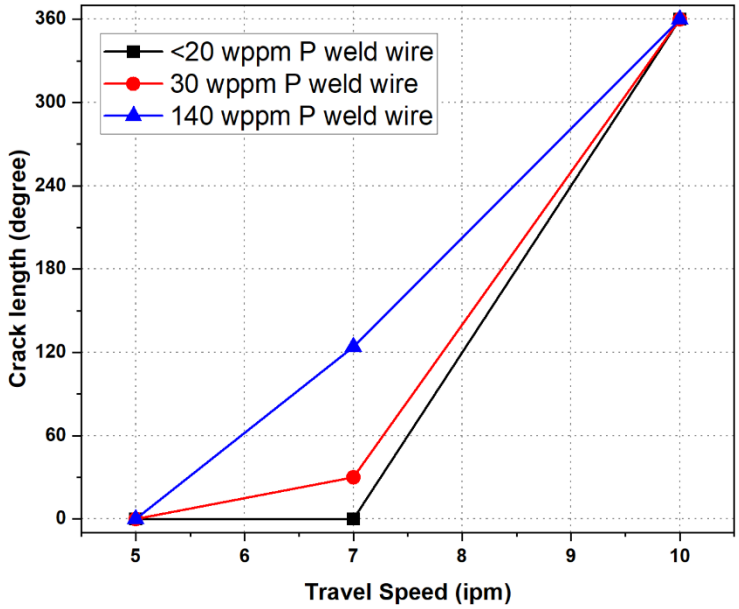

Figure 33. Solidification cracking length as a function of travel speed with three Alloy 709 weld wires.

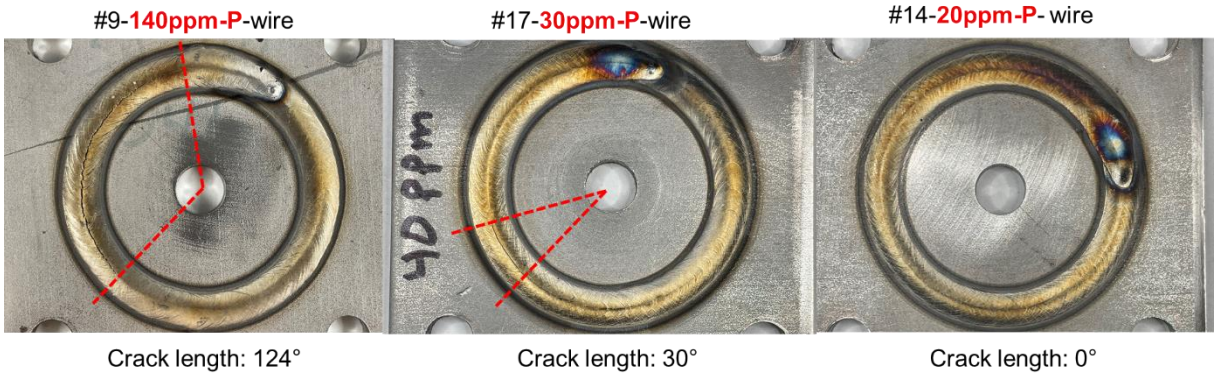

Figure 34. Top view of the centerline solidification cracking on 304 steel plates with three 709 weld wires (<20 wppm-P, 30 wppm-P, 140 wppm-P).

7. SUMMARY AND FUTURE PLAN

This report summarizes the Alloy 709 welding research conducted in FY 2022 at ORNL. Two Alloy 709 production welds were fabricated on two commercial heats of Alloy 709 plates using matching filler metal with low Phosphorus (P) content of < 20 wppm with gas tungsten arc welding (GTAW). Both production welds successfully passed X-ray inspection, room temperature side-bend testing and tensile testing. This concludes the scale up of the Alloy 709 welding to 2-inch plates with the developed welding procedure. Additional microstructure analysis of both welds did not review solidification cracks, confirming the good quality of these production welds.

A new Alloy 709 weld wire was processed from the Commercial heat-2 plates with 30 wppm of P and was used to fabricate W12 weld on the high P containing Commercial heat-1 plates. This weld passed all weld qualification tests without issues. This study provides confidence to take action in further relaxing the P content in future work.

The preliminary cross-weld creep tests results continue to show little or no creep strength reduction relative to the base metal.

Additionally, experimental setup of circular patch tests has been built at ORNL. The preliminary results on Alloy 709 weld wires with three levels of P show the potential of using this approach for assessing solidification cracking susceptibility of 709 welds.

The research on Alloy 709 weldability in this program so far supports the strategy for successfully welding Alloy 709 having wide range of chemistries without weld solidification cracking. The strategy includes the use of low P level weld wire to weld Alloy 709 having relatively high P. It also includes segregation control and/or stress control welding techniques for P level higher than the above threshold situations. To this end, future R&D plan includes quantitatively determining the threshold or the upper limit of P level that will not cause solidification cracking through systematic (ASTM International, E8-2022, Standard Test Methods for Tension Testing of Metallic Materials, 2022)weldability study, for commonly used arc welding processes such as GTAW, shielded metal arc welding (SMAW), electron-beam welding.

8. BIBLIOGRAPHY

ASME. (2021). *Qualification Standard for Welding, Brazing, and Fusing Procedures; Welders; Brazers; and Welding, Brazing, and Fusing Operators.* ASME Boiler and Pressure Code.

ASME. (2021). *Specification for seamless ferritic and austenitic alloy-steel boiler, superheater, and heat-exchanger tubes.* ASME Boiler and Pressure Code, 2021 Edition.

ASTM International. (2018). *E139-11 Standard Test Methods for Conducting Creep, Creep-Rupture, and Stress- Rupture Tests of Metallic Materials*. Retrieved from www.astm.org.

ASTM International. (2022). *E8-2022, Standard Test Methods for Tension Testing of Metallic Materials.* Retrieved from www.astm.org

Feng, Z., Dai, T., Kyle, D., Wang, Y., & Wang, Y. (2020). *Welding Parameters Optimization and the Fabrication of Qualified Alloy 709 Welds.* ORNL/TM-2020/1706, Oak Ridge National Labaratory, Oak Ridge, TN.

Feng, Z., Dai, T., Kyle, D., Wang, Y., & Wang, Y. (2021). *Report on FY 2021 Fabrication and Testing of Qualified Alloy 709 Welds at ORNL*. ORNL/TM-2021/2171, Oak Ridge National Laboratory, Oak Ridge, TN.

Feng, Z., Vitek, J. M., Liu, T., & Wang, Y. (2018). *Evaluation of the Effect of Alloy Chemistry on the Susceptibility of Weld Solidification Cracking of Alloy 709 Weldment and Development of Mitigation Strategy*. ORNL/TM-2018/965, Oak Ridge National Laboratory, Oak Ridge, TN.

Feng, Z., Wang, Y., Kyle, D., & Dai, T. (2019). *Report on FY19 Fabrication and Evaluation of Weldment for Alloy 709 Commercial Heat Plates.* ORNL/TM-2019/1320, Oak Ridge National Laboratory, Oak Ridge, TN.

Natesan, Natesan, K., Zhang, X., Sham, T.-L., & Wang, H. (2017). *Report on the completion of the procurement of the first heat of Alloy 709.* ANL-ART-89, Argonne National Laboratory, Lemont, IL.

NIPPON STEEL & SUMITOMO STEEL. (2013). *NF709 Material Data Sheet.* Retrieved from http://www.tubular.nssmc.com/product-services/specialty-tube/product/nf709

Sham, T.-L., & Natesan, K. (2017). Code Qualification Plan for an Advanced Austenitic Stainless Steel, Alloy 709, for Sodium Fast Reactor Structural Applications. *International Conference on Fast Reactors and Related Fuel Cycles*, (pp. IAEA-CN-245-74). Yekaterinburg, Russian Federation.

Yamamoto, Y. (2014). Unpublished data. Oak Ridge National Laboratory.

Zhang, X., Sham, T.-L., & Young, G. A. (2019). *Microstructural Characterization of Alloy 709 Plate Materials with Additional Heat Treatment Protocol.* ANL-ART-170, Argonne National Laboratory, Lemont, IL.